Mechanisms Involved in the Removal of Heavy Metals from Stormwater via Lignocellulosic Filtration Media

WA-RD 816.4

Indranil Chowdhury
Yuhao Tian
Mehnaz Shams
Michael Wolcott
Jim Dooley

January 2018

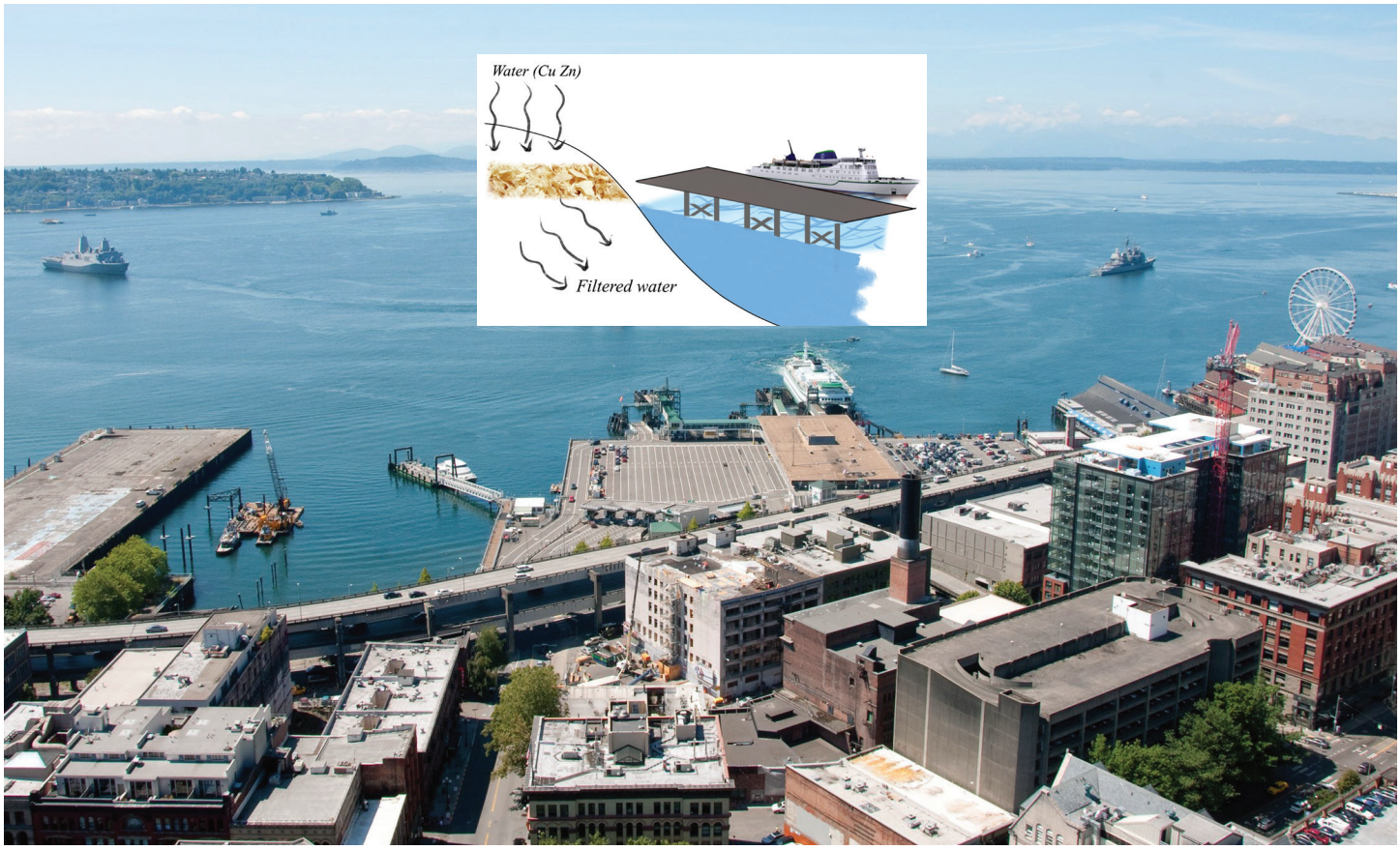

Washington State Department of Transportation
Office of Research & Library Services

WSDOT Research Report

18-03-0115

Research Report

Agreement No. T1462, Task 13 WA-RD 816.4

Mechanisms Involved in the Removal of Heavy Metals from Stormwater via Lignocellulosic Filtration Media

Submitted by:

Indranil Chowdhury, Yuhao Tian, Mehnaz Shams, Michael Wolcott

Department of Civil and Environmental Engineering

Washington State University

Pullman, WA 99164

Jim Dooley

Forest Concepts, LLC

Auburn, WA 98001

Prepared for

The State of Washington

Department of Transportation

Roger Millar, Secretary

January 2018

TECHNICAL REPORT DOCUMENTATION PAGE

1. REPORT NO.	2. GOVERNMENT ACCESSION NO.	3. RECIPIENT'S CATALOG NO.
WA-RD 816.4		

4. TITLE AND SUBTITLE	5. REPORT DATE
Mechanisms Involved in the Removal of Heavy Metals from Stormwater via Lignocellulosic Filtration Media	January 2018
	6. PERFORMING ORGANIZATION CODE

7. AUTHOR(S)	8. PERFORMING ORGANIZATION REPORT NO.
Indranil Chowdhury, Yuhao Tian, Mehnaz Shams, Michael Wolcott, Jim Dooley	

9. PERFORMING ORGANIZATION NAME AND ADDRESS	10. WORK UNIT NO.
Washington State University Department of Civil and Environmental Engineering Pullman, WA 99164-2910	11. CONTRACT OR GRANT NO. Agreement T1462, Task order 13

12. SPONSORING AGENCY NAME AND ADDRESS	13. TYPE OF REPORT AND PERIOD COVERED
Research Office Washington State Department of Transportation Transportation Building, MS 47372 Olympia, Washington 98504-7372 Project Manager: Lu Saechao, SaechaoL@wsdot.wa.gov, 360-705-7260	Final Research Report
	14. SPONSORING AGENCY CODE

15. SUPPLEMENTARY NOTES

This study was conducted in cooperation with the U.S. Department of Transportation, Federal Highway Administration.

16. ABSTRACT:

This report aims to supplement our previous report (Yonge et al. 2016; WA-RD 816.3) that assessed copper and zinc adsorption to lignocellulosic filtration media using laboratory tests and field-scale column tests for urban stormwater remediation. The current project extends the species of wood materials that were investigated in the earlier study. We performed laboratory tests using Douglas-fir crumbles®, poplar crumbles®, tanoak crumbles®, lodgepole pine crumbles®, Ultra-char of poplar®, Ultra-char of alder®, and Ultra-char of Douglas-fir® to evaluate their ability to adsorb copper and zinc. The laboratory column test results indicated that the most efficient adsorption medium for both copper and zinc is ultra-char of poplar, followed by tanoak crumbles, poplar crumbles, ultra-char of Douglas-fir, Douglas-fir crumbles, lodgepole pine crumbles, and ultra-char of alder, in that order. However, the batch experiments showed that tanoak is the most efficient adsorption medium of the samples tested. Based on the summary results of both the column and batch experiments, among all the samples of wood crumbles and char, tanoak crumbles seem to be a better option for metal adsorption. One of the most important conclusions drawn from this project is that the surface areas of both wood crumbles and ultra-chars of different wood crumbles are highly relevant to their ability to adsorb copper and zinc. Building on our previous research, we found that surface area is a critical parameter for copper and zinc removal, and the role of functional groups is not as important as we had expected. Typically, chars have larger surface areas and fewer functional groups than wood crumbles. The presence of functional groups would favor metal adsorption when two materials share similar surface areas, which may explain the superior adsorption performance of raw wood crumbles over char that we reported in our previous report (Yonge et al. 2016).

17. KEYWORDS	18. DISTRIBUTION STATEMENT
Stormwater, Ferry Terminals, Filtration, Copper, Zinc, Washington State	No restrictions. This document is available to the public through the National Technical Information Service, Springfield, VA 22616

19. SECURITY CLASSIF. (of this report)	20. SECURITY CLASSIF. (of this page)	21. NO. OF PAGES	22. PRICE
None	None	48	

Disclaimer

The contents of this report reflect the views of the authors, who are responsible for the facts and the accuracy of the data presented herein. The contents do not necessarily reflect the official views or policies of the Washington State Department of Transportation or the Federal Highway Administration. This report does not constitute a standard, specification, or regulation.

Executive Summary

This report compares the removal efficiency of copper and zinc using a wide range of bio-based filter media in laboratory tests. This work supplements our previous report (Yonge et al. 2016) that assessed copper and zinc adsorption to lignocellulosic filtration media using laboratory tests and field-scale column tests for urban stormwater remediation.

Soluble zinc and copper concentrations that originate from urban stormwater runoff have been reported as a significant threat to native salmon and steelhead populations. In response to negative effects of urbanization, existing stormwater infrastructure needs to be upgraded to treat non-point source pollution, including soluble metals. Effective and low-cost filtration media need to be identified for the removal of such soluble metals from urban runoff.

In the current project, we conducted laboratory tests using Douglas-fir crumbles®, poplar crumbles®, tanoak crumbles®, lodgepole pine crumbles®, Ultra-char of poplar®, Ultra-char of alder®, and Ultra-char of Douglas-fir® to evaluate their effectiveness in adsorbing soluble forms of copper and zinc. The laboratory column test results indicate that the most efficient adsorption medium for both copper and zinc is ultra-char of poplar, followed by tanoak crumbles, poplar crumbles, ultra-char of Douglas-fir, Douglas-fir crumbles, lodgepole pine crumbles, and ultra-char of alder, in that order. However, the batch test results indicate that tanoak has the best adsorption capability among all the wood crumbles and ultra-chars of wood crumbles that were tested. A comparison of the data obtained from the laboratory column tests and the batch experiments suggests that tanoak crumbles are the best option for metal adsorption among all the samples of wood crumbles and chars tested. The column experiments and batch adsorption test results indicate that the surface areas of both the wood crumbles and ultra-chars of different wood crumbles are highly relevant to their ability to adsorb copper and zinc. Furthermore, media with large surface areas showed a propensity to adsorb heavy metal. Lastly, the role of functional groups is not as important as we anticipated.

Contents

List of Tables

List of Figures

1. Introduction and Background

Heavy metals such as copper and zinc that come from worn tires, motor oil, moving engine parts, brake linings, metal platings, de-icing salts, and other anthropogenic sources are of particular concern with regard to stormwater runoff (Brown and Peake 2006; Walker, McNutt, and Maslanka 1999; Angerville et al. 2013; Mahrosh et al. 2014; Gangolli 2007; Davis, Shokouhian, and Ni 2001). These contaminants can be washed into stormwater systems and discharged into lakes, streams, and other waterbodies (Council 2009). Zinc and copper are particular environmental concerns due to their adverse health effects on fish and other aquatic animals (Burton Jr and Pitt 2001; Brooks and Mahnken 2003; Willson and Halupka 1995; Council 2009; Mahrosh et al. 2014; Skidmore 1964).

Filtration is a versatile and simple operation that can be applied to treat contaminated stormwater (Reynolds, Reynolds, and Richards 1996). The most commonly used filtration media for stormwater treatment are sand, crushed rock, gypsum, and dolomite. Many different materials have been tested for heavy metal treatment, such as granular activated carbon (GAC), agricultural waste products, compost, recycled natural fibers, and various biomass-based chars (Chen and Wang 2000; Chen et al. 2011; Demirbas 2008; Yonge and Roelen 2003). Although GAC can adsorb heavy metals effectively, its production and regeneration costs make it less feasible for municipal stormwater treatment than other options (Mohan et al. 2014; Pitcher, Slade, and Ward 2004).

Charcoal is a byproduct of biofuel development and is derived from fast pyrolysis (Mohan, Pittman, and Steele 2006), which is an important pathway to convert lignocellulosic biomass into liquid fuel (Mohan, Pittman, and Steele 2006). Charcoal is the spent carbonized biomass residual (Chen et al. 2011). Charcoal is also called ‘biochar’ when applied for soil amendment and other environmental remediation processes (Ameloot et al. 2013).

In our previous study (Yonge et al. 2016), we conducted laboratory and field-scale column tests to assess copper and zinc adsorption to lignocellulosic filtration media. In that study, Yonge et al. (2016) found that raw crumble® particles worked as well or better than biochar to remove copper and zinc. However, the reason that raw crumbles® worked better than biochar remained unclear. Hence, for the current study, we explored the mechanisms involved in the adsorption of copper and zinc using a wide range of wood crumbles and their respective biochars.

In the previous report (Yonge et al. 2016), the study’s biochar was produced from lodgepole pine, whereas the raw wood sample was from Douglas-fir. Comparisons of the biochar from lodgepole pine and the wood crumbles from Douglas-fir could not explain the reason that the raw wood crumbles showed better adsorption than the biochar. Therefore, in this project, we conducted more comprehensive experiments to explore the relationship between the physicochemical properties of a wide range of wood crumbles and biochars, and their zinc and copper adsorption. We tested Douglas-fir crumbles®, poplar crumbles®, tanoak crumbles®, lodgepole pine crumbles® Ultra-char of poplar®, Ultra-char of alder®, and Ultra-char of Douglas-fir® in our current study. We characterized the surfaces of the raw crumbles® and biochar and analyzed functional groups via Fourier transform infrared

(FTIR) spectroscopy and Brunauer-Emmett-Teller (BET) surface area analysis. This work helped us to compare the surface areas and surface functionalities of various wood crumbles and their role in zinc and copper removal.

After extensive surface characterization, we evaluated the ability of the wood crumbles and biochars to remove zinc and copper using packed-bed filter columns, as follows:

- Regular columns packed with wood crumbles and biochars, similar to those used in the previous study (Yonge et al. 2016).
- Synthetic stormwater used in the previous study.
- Pollutants: zinc and copper.

Findings from the Previous Report (Yonge et al. 2016)

Yonge et al. (2016) performed laboratory and field-scale continuous flow column tests using raw and torrefied Douglas-fir crumbles (*Psuedotsuga menziesii*), charcoal (also referred to as biochar), and pea gravel to evaluate these materials' effectiveness to adsorb soluble forms of copper and zinc. The laboratory column test results indicated that the most efficient adsorption medium for both copper and zinc was non-torrefied wood, followed (in order) by pea gravel, torrefied wood, and charcoal. Increasing the influent column flow by a factor of four resulted in no statistically significant differences in the effluent metal concentrations. A de-icer flush performed on the torrefied wood and charcoal columns following the adsorption tests resulted in an increase of more than an order of magnitude in the column effluent copper and zinc concentrations, indicating that bypassing the filtration system during de-icer runoff events should be considered.

The Bainbridge Island ferry terminal staging area was selected as the field test site. A pilot-scale adsorption column and submersible weir system were designed and constructed to fit within an existing stormwater vault. During each storm event, the column's design allowed stormwater to enter laterally through the top of the column, pass vertically downward through the media, and exit to the submersible weir that was used to determine flow. The performance of the charcoal was tested initially by collecting data from three runoff events. Based on the laboratory performance of the raw wood crumbles, the charcoal was replaced, and data for nine storm events were obtained over the remainder of the field investigation. Column influent and effluent samples were collected during selected stormwater runoff events using automated samplers. The samples were analyzed for soluble and total copper and zinc, total and volatile suspended solids, and pH. Column flow and rainfall data also were collected during the field investigation. The data indicated that, overall, the raw wood crumbles yielded a higher percentage of soluble metal removal and lower metal concentrations compared to the charcoal. The field data do support the findings of the laboratory column tests; however, the raw wood crumbles yielded a higher percentage of removal and lower effluent soluble copper and zinc concentrations compared to charcoal.

2. Experimental Methods

For this study, we conducted column experiments and adsorption batch tests to evaluate the effectiveness of Douglas-fir crumbles®, Poplar crumbles®, Tanoak crumbles®, Lodgepole pine crumbles®, Ultra-char of poplar®, Ultra-char of alder®, and Ultra-char of Douglas-fir® in removing copper and zinc from synthetic stormwater.

2.1 Media Preparation

Woody Biomass Sample Preparation

The woody biomass materials used in this study were produced by Forest Concepts, LLC of Auburn, WA. The poplar and Douglas-fir samples came from western Washington, tanoak from northern California, and lodgepole pine was from northern Colorado. Round logs of each species were converted by Forest Concepts to rotary veneer using a centerless lathe. The veneer thickness was set to equal the nominal particle size of 2 mm or 4 mm as desired. Round-up veneer containing bark and cambium was discarded. Clean veneer from the interior of the logs was then fed cross-grain into a Forest Concepts Crumbler® rotary shear machine to produce uniform flowable particles (Dooley, Lanning, and Lanning 2013). The 2-mm nominal particles were sheared with a cutter head having 1.6-mm cutter thickness, and the 4-mm nominal particles were sheared with a cutter head having 4.8-mm cutter thickness. After milling, the output of the rotary shear machine was screened using a two-deck Forest Concepts Model 2448 orbital screen. The screen openings were used to sieve each material. After processing, the final materials were dried in a tray-type dryer at 50ºC to a moisture content of approximately 10 percent (weight basis (wb)) before being packaged in polyethylene bags for storage.

Biochar Samples Preparation

The rotary-sheared wood particles were converted to biochar in a propane-heated retort. Approximately 3 liters of dry (typically 10% wb) particles were placed into a cast-iron pan with a tight-fitting cast-iron lid. The pan was 40 cm long, 30 cm wide, and 5 cm deep. The raw biomass material occupied approximately one-half the volume of the pan and airspace under the lid. The pan was placed on a grate over a multi-port propane burner inside housing that was approximately 80 cm long, 50 cm wide, and 20 cm tall. The temperature within the housing was maintained at approximately 275ºC to 300ºC until all the material was uniformly converted to biochar. Since the propane burner was directly beneath the cast-iron pan, the temperature of the interior of the pan was measured to be approximately 320ºC to 350ºC. The tray was carefully opened after approximately 30 minutes, and then every 15 minutes to inspect the degree of charring. The biochar was deemed complete when all particles were pure black and had a uniform chunk-charcoal-like appearance. Due to differences in species, particle size, and the ambient environment around the retort, the time to completion sometimes can be highly variable and range from 45 minutes to over two hours. Upon completion of the roasting stage, the tray was removed from the housing and allowed to air cool to less than 100ºC. At that point, the contents were dumped onto a steel pan in a thin layer where the material was sprayed with fresh water until it no longer produced steam. The material was fully cooled in ambient air before being packaged.

2.2 Media Screening

All wood materials were screened, and basic properties were measured; see Table 1.

Table 1. Basic Description of Wood-Based Materials

#	Sample	ID	Size	Pass	No Pass	Moisture Content
1	Poplar	2013.03.28.001	2 mm	3/16”	No. 20 orbital screen	5%
2	Douglas-fir	2012.02.09.001.A.A.A.A	2 mm	3/16”	No. 20 orbital screen	5%
3	Tanoak	2014.03.03.001.A.A.B	2 mm	3/16”	No. 20 orbital screen	5%
4	Lodgepole pine	2012.12.12.001.A	4 mm	3/8”	3/32”	5%
5	Ultra-char poplar	2014.12.28.003	2 mm	3/16”	No. 20 orbital screen	Dry
6	Ultra-char alder	2016.01.11.01	4 mm	3/8”	3/32”	Dry
7	Ultra-char Douglas-fir	2016.01.20.03	2 mm	3/16”	No. 20 orbital screen	Dry

2.3 Fourier Transform Infrared Spectroscopy Analysis

An FTIR spectrum was obtained from 4000 cm^{-1} to 500 cm^{-1} for each wood sample. The samples were ground in a mortar and pestle and then added to FTIR grade potassium bromide. The raw wood samples were analyzed at a concentration of 2.5 percent, and the ultra-char samples were analyzed at a concentration of 1 percent. The samples were analyzed using a Thermos Nicolet Nexus 670 FTIR spectrometer.

2.4 Surface Area Measurements

The surface areas of the wood crumbles and biochar samples were analyzed using a Tri-Star 3000 BET surface area analyzer at the W. M. Keck Biomedical Materials Research Laboratory at Washington State University (WSU).

2.5 Density Measurements

On a 4-place balance, approximately 1 g was weighed out and placed into a 50-mL graduated cylinder that was already filled with 30 mL of Milli-Q water at 20ºC. The cylinder was sealed and inverted to make sure that all the wood samples were hydrated, and then the cylinder was placed on the counter before reading the displaced volume.

2.6 Chloride Analysis

Synthetic surface water amended with a 70:30 roadway de-icer mixture of NaCl and $MgCl_2$ was prepared in a 20-L high-density fluorinated polyethylene container. The de-icer amended synthetic surface water was prepared by adding 0.338 g of $MgSO_4 \cdot 7H_2O$, 0.065 g of $KHCO_3$, 0.725 g of $NaHCO_3$, 0.664 g of $CaCO_3$, 34.331 g of NaCl, and 51.891 g of $MgCl_2 \cdot 6H_2O$ to 20 L of Milli-Q H_2O. The chloride amended synthetic surface water was then pumped at 6 mL/min into a 15-mm ID x 150-mm glass column with 2 g of each wood sample tested and 30 μm polytetrafluoroethylene frits on both ends. Ninety fractions were collected over 90 minutes using a Spectrum Labs CF-1 fraction collector in clean glass 8-

mL vials. The chloride was analyzed using a Seal Analytical AQ-400 discreet analyzer and method EPA-105-C.

Figure 1 shows two columns packed with poplar and Douglas-fir wood sample materials. Figure 2 shows the whole column test system set-up.

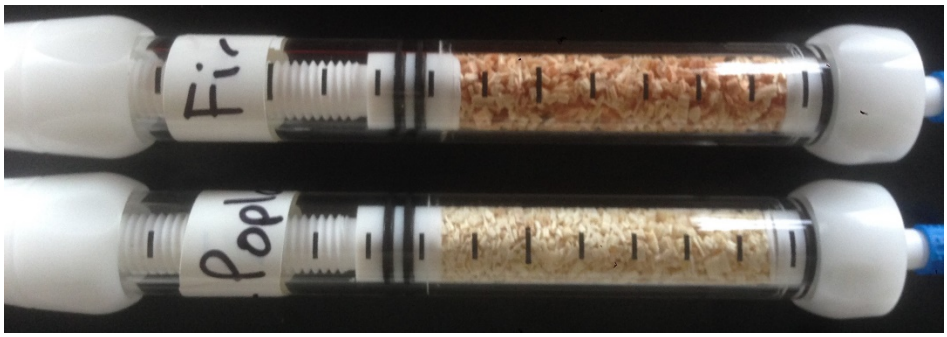

Figure 1. Photo of packed columns of Douglas-fir and poplar wood crumble samples.

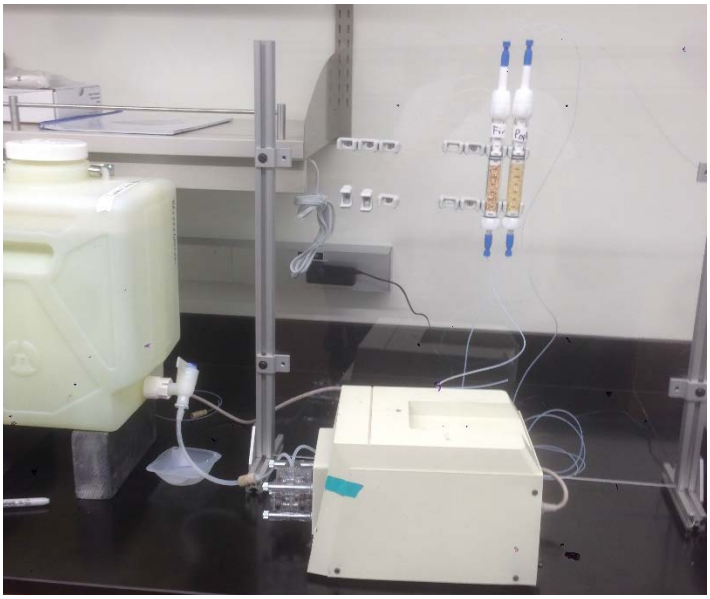

Figure 2. Photo of column test system set-up.

2.7 Alkalinity Analysis

Alkalinity was analyzed for all the chloride samples running through each wood column using Seal Analytical AQ-400 and method EPA-101-A.

2.8 pH Value Measurements

After the chloride and alkalinity analyses, the pH values were measured for pairs of column fractions using a pH meter (Orion™ Versa Star Pro™ pH Benchtop Meter) purchased from Fisher Scientific. Sample pairs (minutes 1 and 2, 3 and 4, etc.) were combined to provide

sufficient sample volumes.

2.9 Adsorption Experiment

Synthetic stormwater was made in 5-L batches and stored in high-density polyethylene containers. Deionized (DI) water was used as the foundation for the batch synthetic stormwater. Individual metal stock solutions (1000 mg/L) of copper and zinc were made using reagent grade, granular cupric chloride dihydrate ($CuCl_3.2H_2O$) and zinc chloride ($ZnCl_2$) (Fisher Scientific). The DI water was spiked with a known volume of each stock solution to achieve target influent concentrations of 300 μg/L zinc and 100 μg/L copper. The pH of the synthetic stormwater was adjusted to 6.1 by NaOH stock solution made from reagent grade sodium hydroxide pellets (J. T. Baker). A Hach® benchtop pH meter combined with an IntelliCALTM Ultra Refillable pH probe, designed for low ionic strength samples, was used to measure the pH. The synthetic stormwater solution was mixed for one minute using a polyvinyl chloride rod and allowed to equilibrate for a minimum of 12 hours before use. Following the equilibrium period, the pH was checked to assure that it was within the desired range. All other operation conditions are the same as described in Section 2.6.

2.10 Adsorption Equilibrium Tests

Single-solute and multi-solute equilibrium adsorption isotherm data were generated for all seven wood materials, with zinc and copper as the sorbates. The data were generated at room temperature (20°C ± 1°C) using a series of 15-mL polypropylene tubes. All tubes contained a known mass of sorbent, solution volume, and initial concentration of sorbate. The tubes were shaken and kept for 24 hours before they were analyzed for soluble metal concentration.

Copper and zinc stock solutions (1000 mg/L) were prepared using reagent grade copper chloride ($CuCl_2$) and zinc chloride ($ZnCl_2$) (Fischer Scientific) dissolved in 18-MΩ DI water. The stock solutions were diluted with DI water that contained 0.01-M $NaNO_3$, yielding a typical ionic strength found in stormwater, to a volume of 15 mL at predetermined sorbate concentrations. A known mass of sorbent and a predetermined volume of 1 M NaOH or 1 M HNO_3 were added to each bottle so that the pH value following equilibration would be between 6.0 and 6.5. Table 2 presents the initial liquid phase metal concentrations and sorbent mass values for the single-solute and multi-solute systems.

Table 2. Initial Liquid Phase Metal Concentrations and Sorbent Masses Used For Single-Solute and Multi-Solute Systems

Metal	Target Metal Conc. (mg/L)	Sorbent Mass (mg)
Single-solute, copper	Copper: 0.7	100, 200, 300, 400, 500
Single-solute, zinc	Zinc: 0.1	100, 200, 300, 400, 500
Multi-solute, copper and zinc	Copper: 0.25; zinc: 0.45	100, 200, 300, 400, 500

For both the single- and multi-solute systems, triplicate control bottles were tested using previously stated procedures but without sorbent. The results indicated negligible sorption to the bottle walls.

The liquid phase metal concentrations were measured using an inductively coupled plasma-mass spectrometer (ICP-MS) at WSU (Pullman, WA) using a NexION 350x ICP-MS (Perkin Elmer, Inc.). Before analysis, all samples were filtered through a 0.45-μm filter and acidified to a pH value less than or equal to two.

Following quantification of the liquid phase sorbate concentration, the solid phase sorbate concentration was calculated using Equation 1,

$$q_e = \frac{(C_o - C_e)V}{m} \quad (1)$$

where q_e is the equilibrium solid phase concentration (mg sorbate/g sorbent), C_e is the equilibrium liquid phase concentration (mg/L), C_o *i*s the initial liquid phase concentration (mg/L), *V* is the sorbate volume (L), and *m* is the mass of the sorbent (g).

2.11 ICP-MS Analysis of Zinc and Copper

Measurements were carried out using a PerkinElmer ICP-MS NexION 350X system. High purity HNO_3 (Arista Ultra, for ultra-trace metal analysis, BDH, VWR Analytical, Philadelphia, PA) was used as received for sample acidification. Deionized water was collected from a Milli-Q system. Mixed standard solutions of copper and zinc were prepared from a 100-mg/L multi-element solution (ARISTA, ICP Standard, BDH, VWR Analytical, Philadelphia, PA). All prepared standard solutions were acidified with HNO_3 (1% in final solution). Aqueous standard solutions covering the concentration range (copper 0-100 μg/L, zinc 0-500 μg/L) were used for external calibration. Four standards were used for each element, thus providing correlation coefficients that were greater than 0.999. Standards were prepared daily in a flow hood.

2.12 Data Analysis

Statistical testing was employed for data analysis. When needed, one-sample t-tests and two-sample t-tests for hypothesis testing were conducted using OriginPro 2016 software (OriginLab Corporation, MA) to guarantee the statistical significance of the conclusions.

3. Results and Discussion

3.1 Density and Surface Area

Table 3 shows the measured density values and surface areas of all the wood materials used in the experiments. The surface areas of the wood samples were analyzed using the BET surface area analyzer described in Section 4. Although the BET analyzer has a few limitations when measuring the surface area of wood samples due to wood's porous and biological structure (Lange et al. 2016), we utilized the BET analyzer to get a comparative idea regarding the surface areas of all the wood crumbles and biochar samples. Table 3 lists the density values of the different media and compares them with those reported in the literature. The ultra-chars show lower density values than most of the raw wood crumbles. As for surface area, the wood crumbles share similar surface areas of around 0.5 m^2/g. The ultra-chars have greater surface areas except for the alder char.

Table 3. Characterization of Different Wood Materials

#	Sample (size)	Measured Density (g/cm^3)	Literature Density (g/cm^3)	Surface Area (m^2/g)
1	Poplar crumbles 2 mm	0.5037	0.35-0.50	0.5117
2	Douglas-fir crumbles 2 mm	NA	0.53	0.3377
3	Tanoak crumbles 2 mm	NA	0.58	0.5083
4	Lodgepole pine crumbles 2 mm	NA	0.38-0.62	0.4356
5	Ultra-char poplar 2 mm	0.29	NA	0.9068
6	Ultra-char alder 4 mm	0.27	NA	0.3033
7	Ultra-char Douglas-fir 2 mm	0.513	NA	25.817

3.2 Fourier Transform Infrared Spectroscopy Analysis Results

Figure 3 and Figure 4 present the FTIR spectroscopy results for the wood crumbles and ultra-chars of different woods, respectively. Differences in the peak intensity of the different wood-based materials indicate different functional group intensity (Colom et al. 2003; Park et al. 2013). The figures suggest that those materials share some common functional groups, such as O-H (stretching frequency from 3200 cm^{-1} to 3650 cm^{-1}) and C-H (2700 cm^{-1} to 3200 cm^{-1}) bonds. The signal intensity values of the O-H and C-H bonds of the different woods are different. For the O-H bonds, the signal intensity order is as follows: poplar > tanoak > Douglas-fir > lodgepole pine. The ultra-chars show weak signals in the O-H bonds.

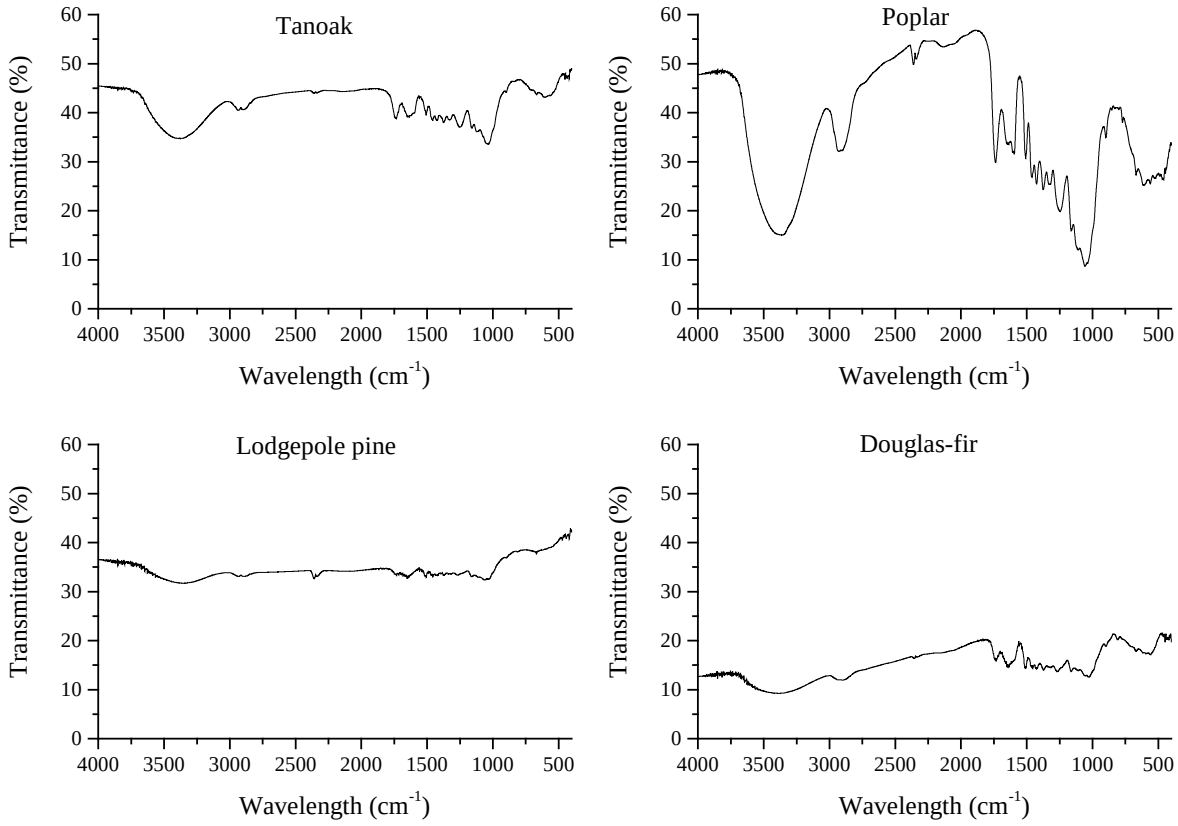

Figure 3. FTIR spectra of various wood crumbles.

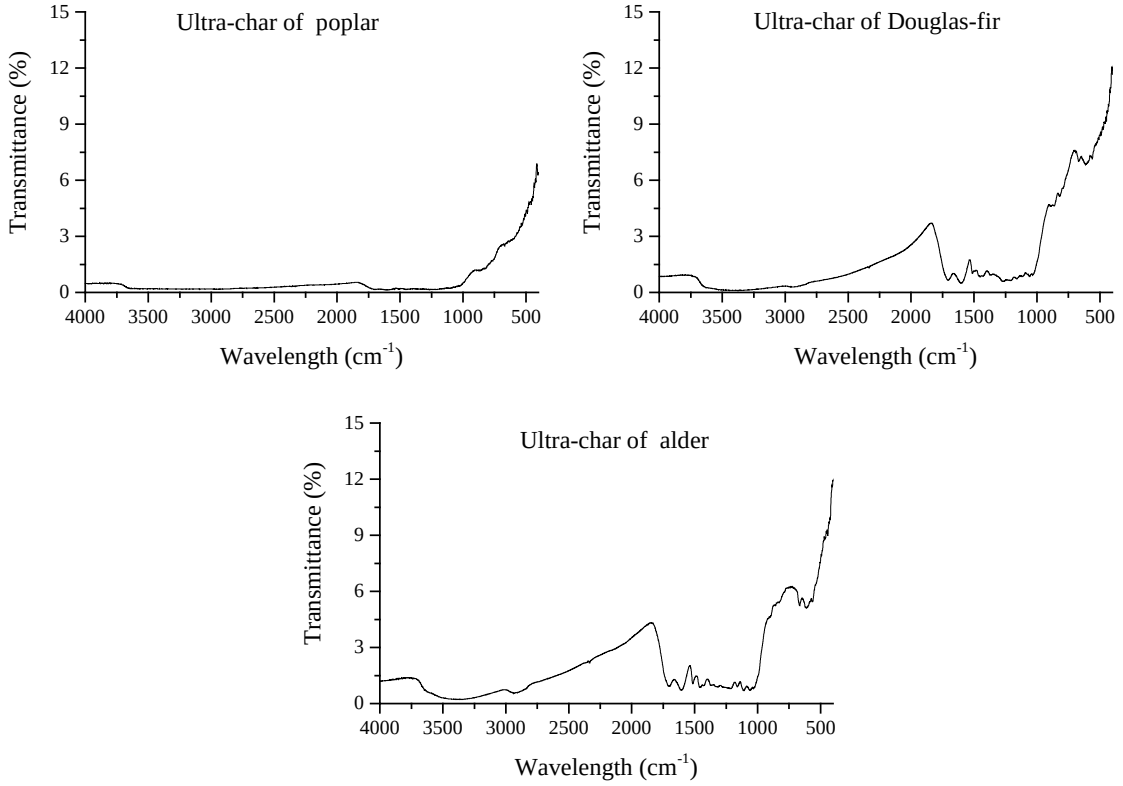

Figure 4. FTIR spectra of various ultra-chars.

In a previous study (Park et al. 2013), FTIR spectra of different materials were provided between 1900 cm^{-1} to 900 cm^{-1} to study guaiacyl rings (1510 and 1600 cm^{-1}), aliphatic C-O-C (1050 cm^{-1}), carbonyl (R-COR') (1740 cm^{-1}), and carboxylic acid (1700 cm^{-1}). Figure 5 presents the structure of units of lignin. In this study, all the structures mentioned above agree with the findings from the (Park et al. 2013) study in that the peaks are more intense for raw wood than for biochars. In the Park et al. (2013) report, the differences in the functional groups of raw wood and biochar played a more important role in the adsorption of heavy metal than in this study.

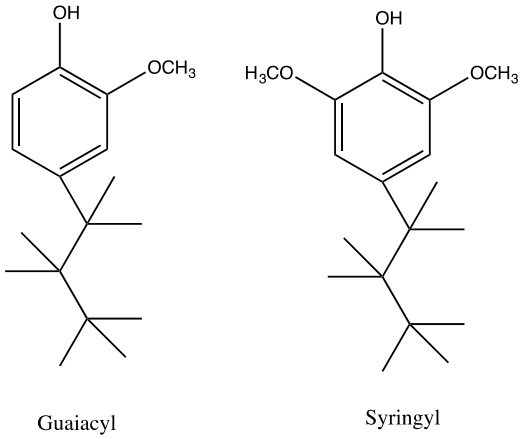

Figure 5. Schematic illustration of building units of lignin (Demirbas 2008).

Tanoak is reported to be an important source of tannic acid for tanning (Bowcutt 2015). As shown in Figure 6, tannic acid possesses a large number of OH functional groups, which could be advantageous for copper and zinc adsorption.

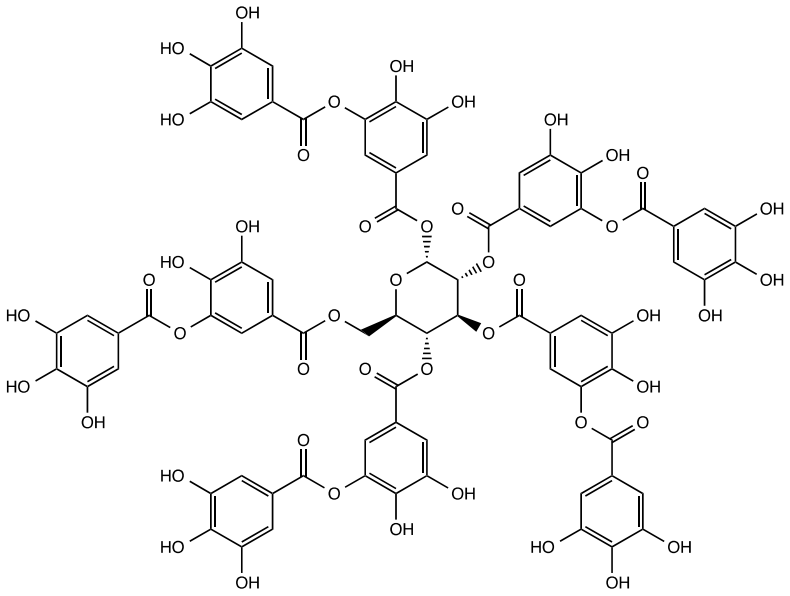

Figure 6. Schematic illustration of tannic acid (Bowcutt 2015).

3.3 Chloride Analysis Results

Chloride shows no differences for all wood-based materials, which makes it an excellent tracer for analysis. Hence, chloride analysis has been used as the control experiment for this study. Figure 7 shows that the chloride concentrations did not change for the different

kinds of wood crumble columns.

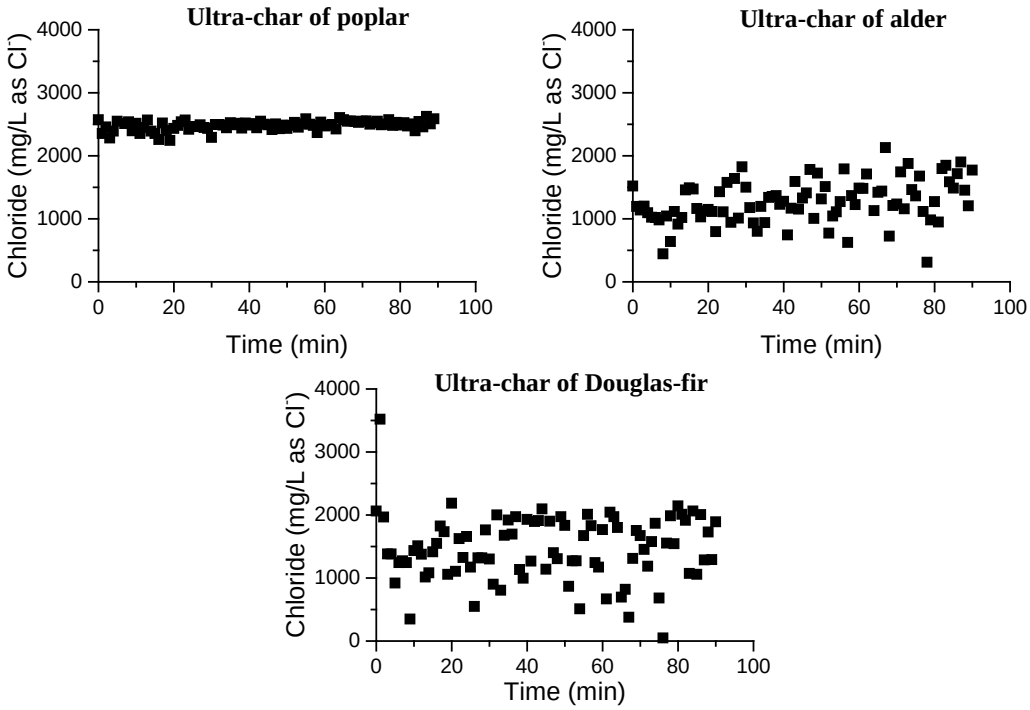

Figure 8 shows similar results to those in Figure 7, where the chloride concentrations did not change during the adsorption experiments.

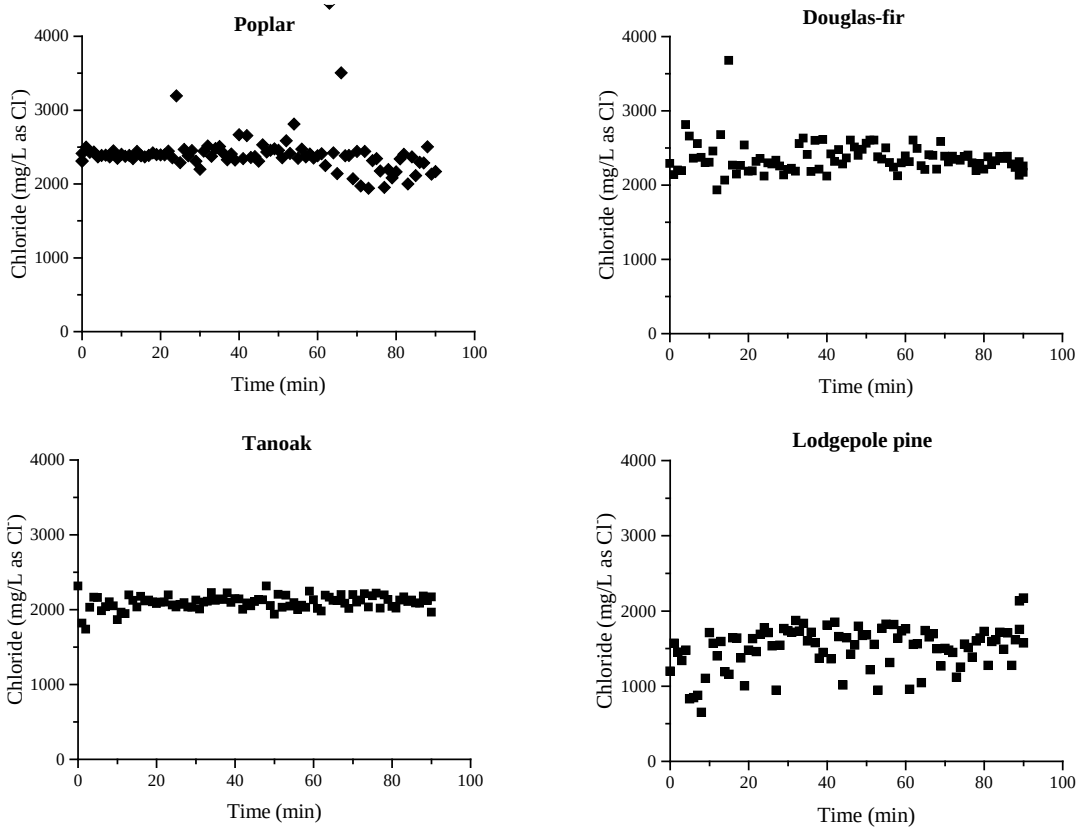

Figure 7. Chloride experiments with wood crumbles.

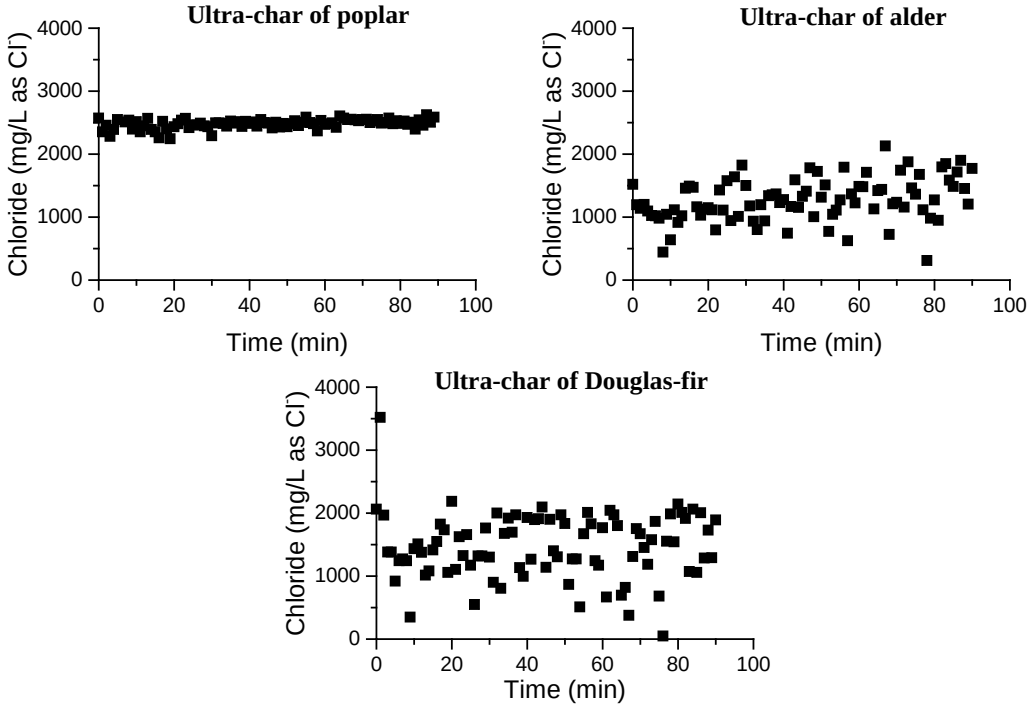

Figure 8. Chloride experiments with ultra-chars.

3.4 Alkalinity and pH Changes during Experiments

Figure 9 and Figure 10 show that the pH and alkalinity values increased gradually during the experiments. The pH decreased at the beginning and then increased gradually in the crumbled wood experiments. In the ultra-char experiments, however, the pH values showed less change. This phenomenon may be related to the amine, nitrile, or other basic functional groups in the different wood materials. Hence, wood-based filtration media needs to be equilibrated prior to usage as filtration media for removal of heavy metals in the ferry terminal.

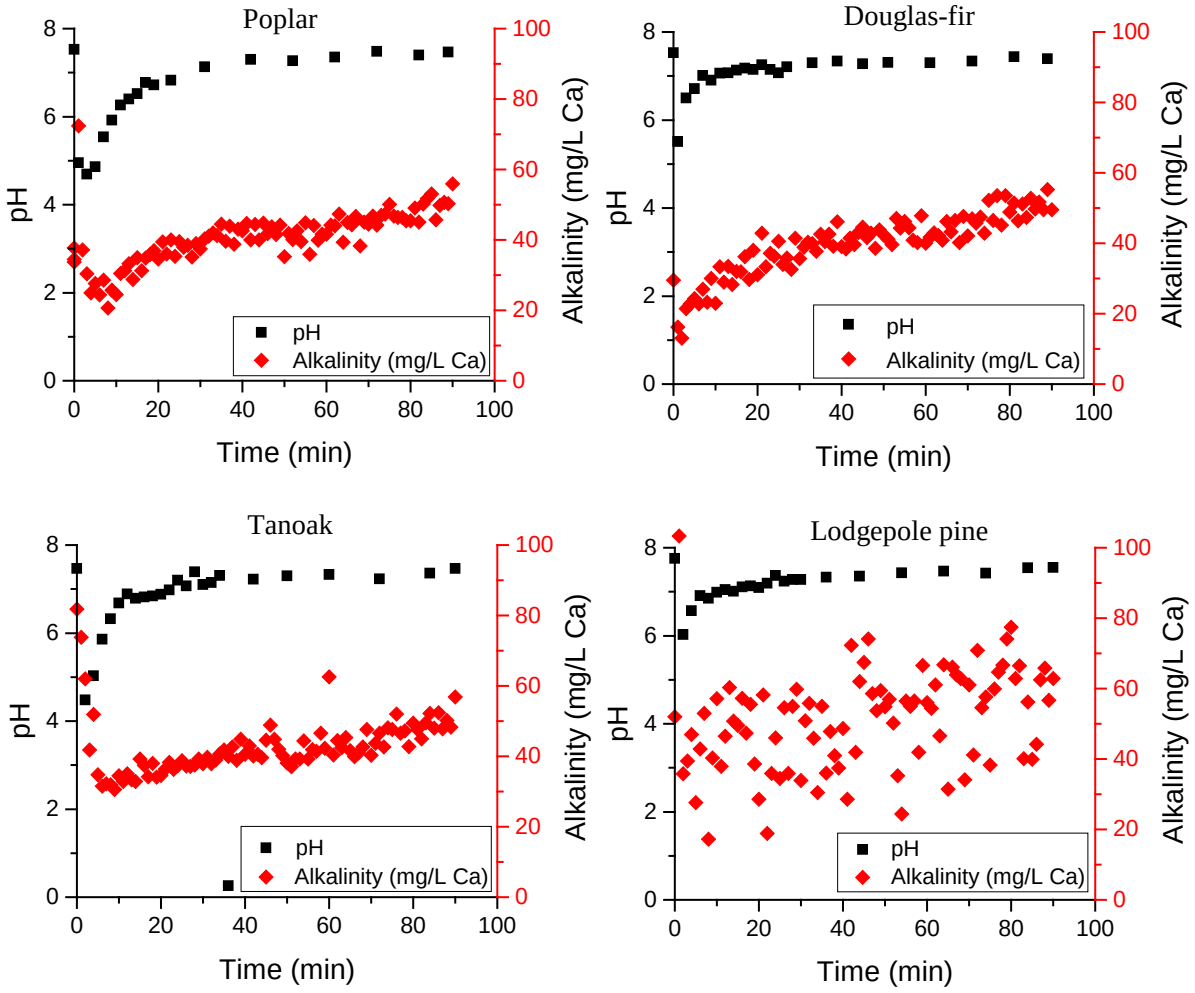

Figure 9. pH and alkalinity values during experiments with wood crumbles.

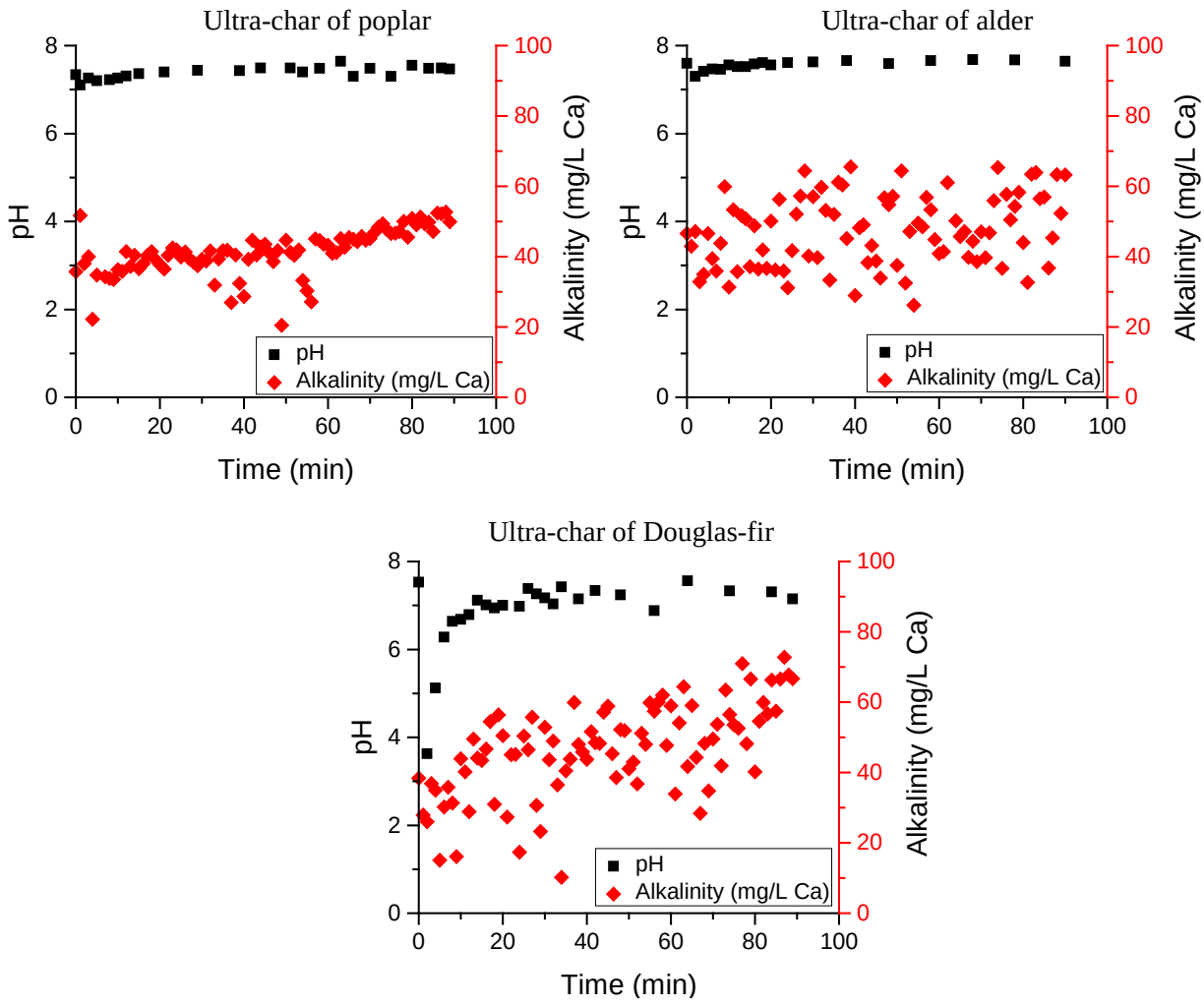

Figure 10. pH and alkalinity values during experiments with ultra-chars.

3.5 Zinc and Copper Adsorption Results

Figure 11 and Figure 12 present the calibration curves for zinc and copper, respectively. The concentration range for zinc is 0 µg/L to 500 µg/L and for copper is 0 µg/L to 100 µg/L. The detection limits for zinc and copper are 0.06 ppb and 0.035 ppb, respectively. The zinc and copper concentrations in the column effluent were calculated based on the calibration curves presented in Figures 11 and 12.

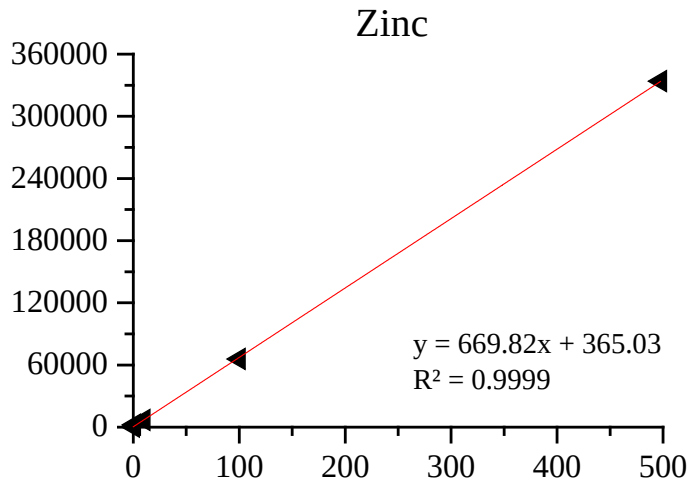

Figure 11. Calibration curve for zinc.

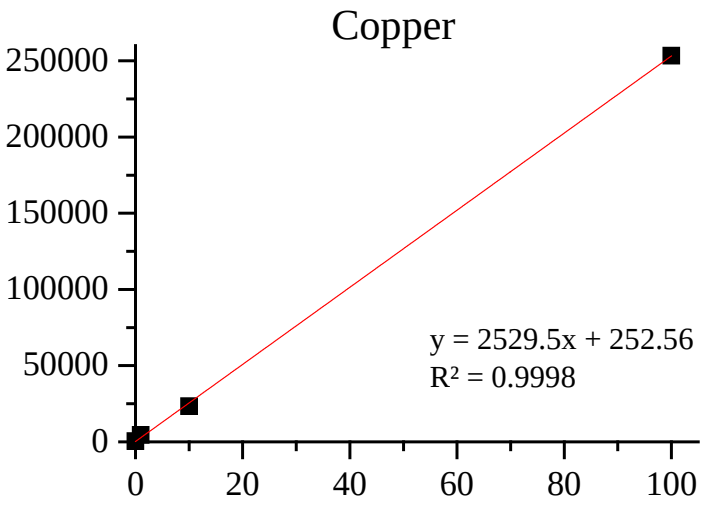

Figure 12. Calibration curve for copper.

3.5.1 Comparison of copper and zinc in effluent from various wood-based columns

Copper concentration in column effluent

Douglas-fir and ultra-char of Douglas-fir

Figure 13 shows the copper concentrations in the effluent of columns packed with Douglas-fir and ultra-char Douglas-fir. Figure 13 shows that the copper concentration in both the Douglas-fir crumbles and the ultra-char of Douglas-fir decreased at the beginning, then increased slowly. The ultra-char shows slightly better adsorption than the Douglas-fir crumbles initially (95% confidence with p-value < 0.05). However, after one hour, the adsorption performance between the Douglas-fir crumbles and ultra-char was negligible. This phenomenon could be explained by the difference in the functional groups of Douglas-fir and ultra-char of Douglas-fir. The overall adsorption differences between the Douglas-fir crumbles and Douglas-fir ultra-char may stem from their density instead of from their

chemical properties. Based on the FTIR spectroscopy results shown in Figure 3, ultra-char of Douglas-fir shows fewer OH and CH functional groups than Douglas-fir crumbles. Ultra-char has a greater surface area than Douglas-fir crumbles, as shown in Table 3. The adsorption results indicate that ultra-char adsorbs more copper than Douglas-fir crumbles (95% confidence with p-value < 0.05). Therefore, for copper adsorption with Douglas-fir crumbles and ultra-char of Douglas-fir, the functional groups play less important roles than the surface areas. As time elapsed, the difference between the Douglas-fir and Douglas-fir ultra-char lessened. Therefore, the cost of materials needs to be considered for actual practical applications.

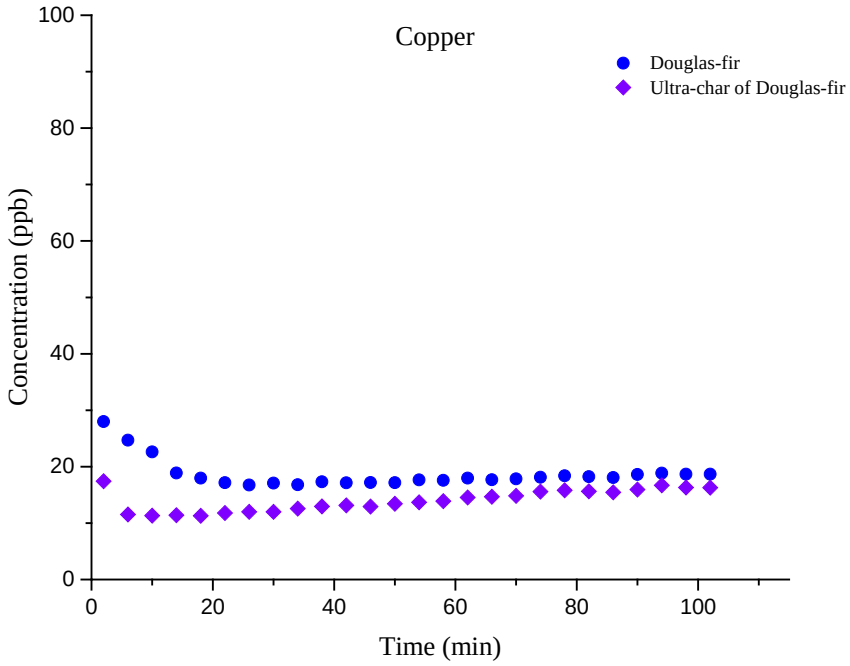

Figure 13. Copper concentration in column effluent: Douglas-fir and ultra-char of Douglas-fir.

Poplar and ultra-char of poplar

Figure 14 shows the copper concentrations in the effluent of the poplar and poplar ultra-char columns. Figure 14 shows that the copper concentrations for both the poplar and poplar ultra-char decreased initially. However, after 30 minutes, the effluent copper concentrations did not change significantly. A possible reason for this outcome could be the release of copper from the poplar crumbles and ultra-char of poplar, or perhaps the crumbles reached a saturation point and the adsorption rate could not increase further. Overall, the ultra-char of poplar shows better adsorption performance than the poplar crumbles. As time elapsed, the difference between the poplar crumbles and poplar ultra-char lessened. The ultra-char has a greater surface area and fewer functional groups than the poplar crumbles. For copper adsorption with poplar crumbles and poplar ultra-char, the

surface area seems more important than the functional groups.

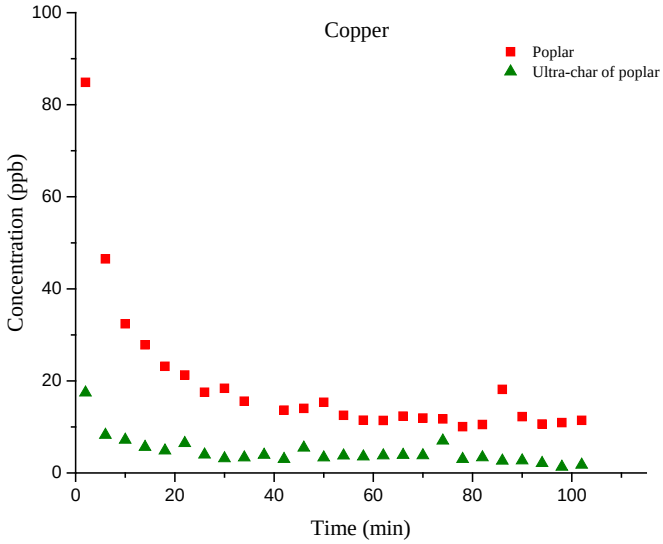

Figure 14. Copper concentration in column effluent: poplar and ultra-char of poplar.

Tanoak, lodgepole pine, and ultra-char of alder

Figure 15 shows the copper concentrations in the effluent of tanoak, lodgepole pine, and ultra-char of alder columns. Figure 15 shows that the copper concentration in both the tanoak crumbles and pine crumbles decreased at the beginning, then stayed at low concentrations. The copper concentration in the tanoak effluent is the lowest of the three columns, and the ultra-char of alder effluent has the highest copper concentration. These results indicate that tanoak is better at copper adsorption than pine, followed by alder ultra-char. Table 3 also shows that tanoak has the greatest surface area and ultra-char of alder has the lowest surface area of these three samples, which match our column results as well.

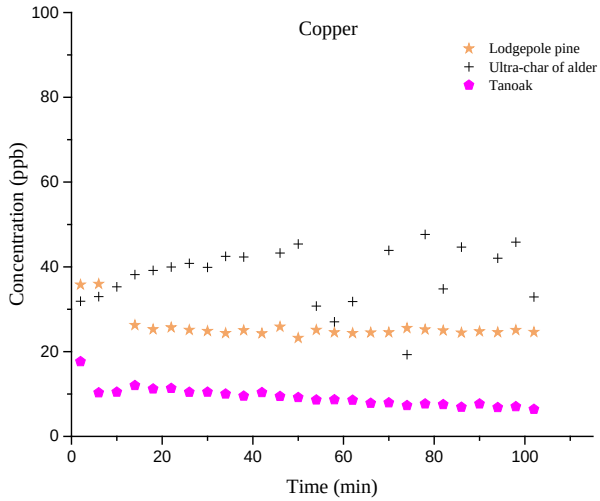

Figure 15. Copper concentrations in column effluent: tanoak, lodgepole pine, and ultra-char of alder.

Zinc concentration in column effluent
Douglas-fir and ultra-char of Douglas-fir

Figure **16** shows the zinc concentration in the effluent of Douglas-fir and ultra-char of Douglas-fir. The zinc concentration is lowest at the beginning and slowly increased during the 100-minute sampling time (95% confidence with p-value < 0.05).
Figure **16** shows that the zinc concentration in the Douglas-fir effluent is lower than in the ultra-char effluent; this finding suggests that Douglas-fir crumbles adsorb zinc better than the ultra-char of Douglas-fir. This may be due to higher amount of functional groups for Douglas-fir crumbles. This outcome is the opposite to that of copper effluent for these two wood columns.

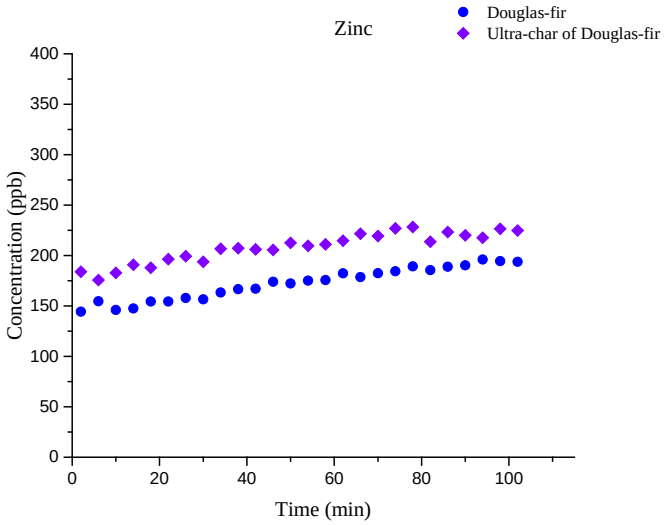

Figure 16. Zinc concentration in column effluent: Douglas-fir and ultra-char of

Douglas-fir.

Poplar and ultra-char of poplar

Figure 17 shows the zinc concentration in the effluent of the poplar column and the ultra-char of poplar.

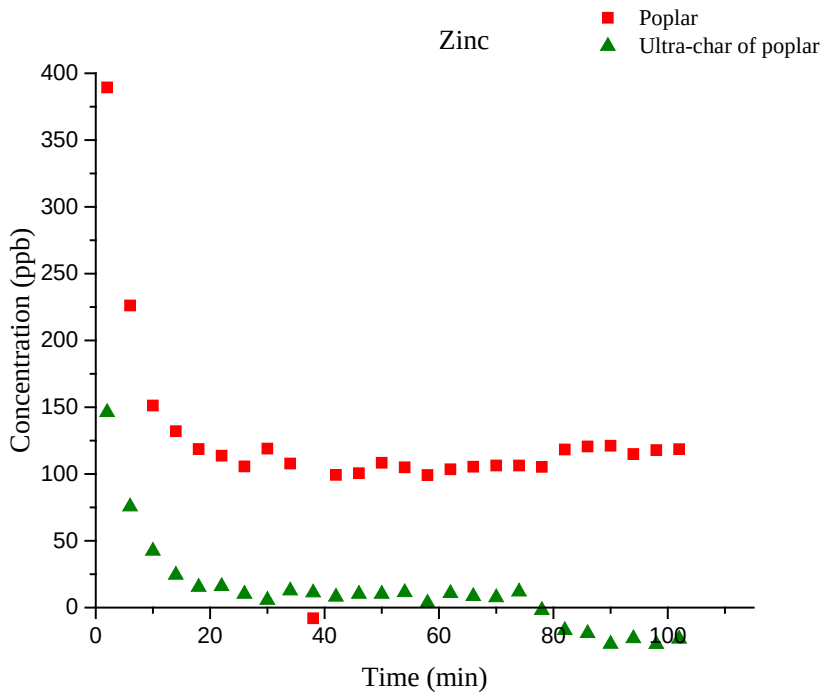

Figure 17. Zinc concentration in column effluent: poplar and ultra-char of poplar.

Figure 17 shows that the zinc concentrations in both the poplar crumbles and the poplar ultra-char decreased for the first few minutes and then stayed at constant concentrations, similar to the copper concentrations. In this case, the ultra-char of poplar adsorbed zinc better than poplar because the concentration of zinc in the effluent is much lower than that in the poplar column effluent. It appears that almost all the zinc was absorbed by the ultra-char of poplar. This result is similar to that for the copper effluent in these two wood columns. Both poplar crumbles and ultra-char of poplar show better zinc adsorption than Douglas-fir and ultra-char of Douglas-fir (t-test, 95% confidence with p-value < 0.05). However, from the FTIR spectroscopy results shown in Figure 3, poplar crumbles have more OH and CH functional groups than the Douglas-fir crumbles. Table 3 also shows that poplar crumbles have greater surface areas than Douglas-fir crumbles. However, ultra-chars of poplar have fewer OH functional groups than poplar crumbles. But surface area of ultra-char of poplar is almost two times higher than poplar crumbles. Ultra-char of poplar performs better in zinc adsorption than poplar crumbles. Therefore, surface area seems more important than functional groups for zinc adsorption.

Tanoak, lodgepole pine, and ultra-char of alder

Figure 18 shows the zinc concentrations in the effluent of tanoak, lodgepole pine, and ultra-char of alder columns. Figure 18 shows that the zinc concentration in the tanoak effluent is

the lowest of the three columns tested, followed by the effluent from pine. The ultra-char of alder effluent is the highest concentration, which means that tanoak adsorbs zinc better than pine, and pine adsorbs zinc better than ultra-char of alder, which is similar to the results for copper adsorption. Table 3 also shows that, among these three samples, tanoak has the greatest surface area and ultra-char of alder has the smallest surface area; these results match our results as well.

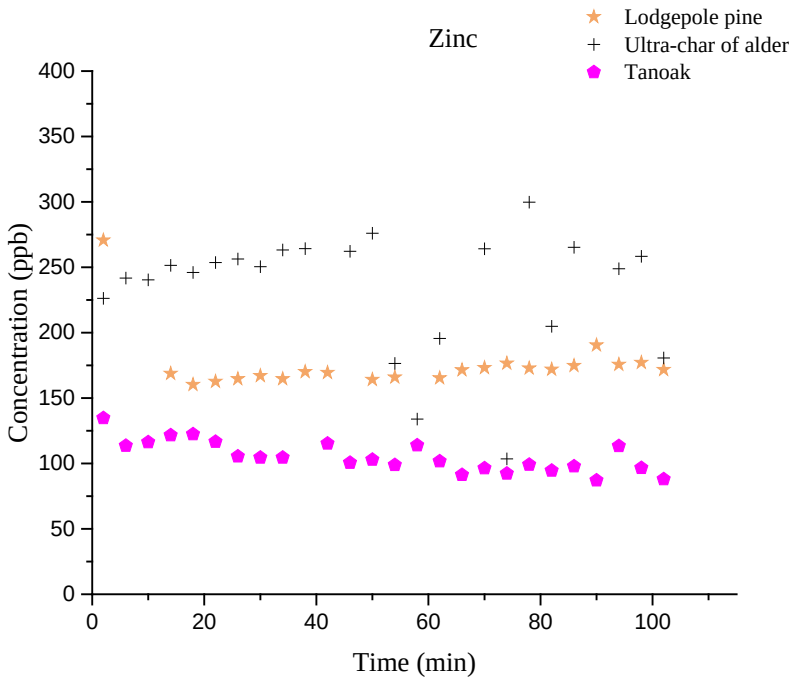

Figure 18. Zinc concentrations in column effluent: tanoak, lodgepole pine, and ultra-char of alder.

Figure 19 shows the regression analysis results for the copper and zinc concentrations in the column effluent at 60 minutes to the surface area and the OH functional group (the OH functional group is the most dominant functional group according to the FTIR spectrometry results shown in Figure 3). Figure 19 shows that, for all six wood-based materials, the copper and zinc concentrations in the effluent decreased with a greater surface area. In the case of the functional groups, more OH functional groups resulted in lower copper and zinc concentrations in the column effluent. However, the surface area plays a more important role in copper and zinc adsorption than the functional groups. For example, ultra-char of poplar, which has almost no functional group signal, removes zinc and copper the best of these samples due to its large surface area. Overall, the results obtained from the column tests indicate that ultra-char of poplar might be the best choice for copper and zinc adsorption.

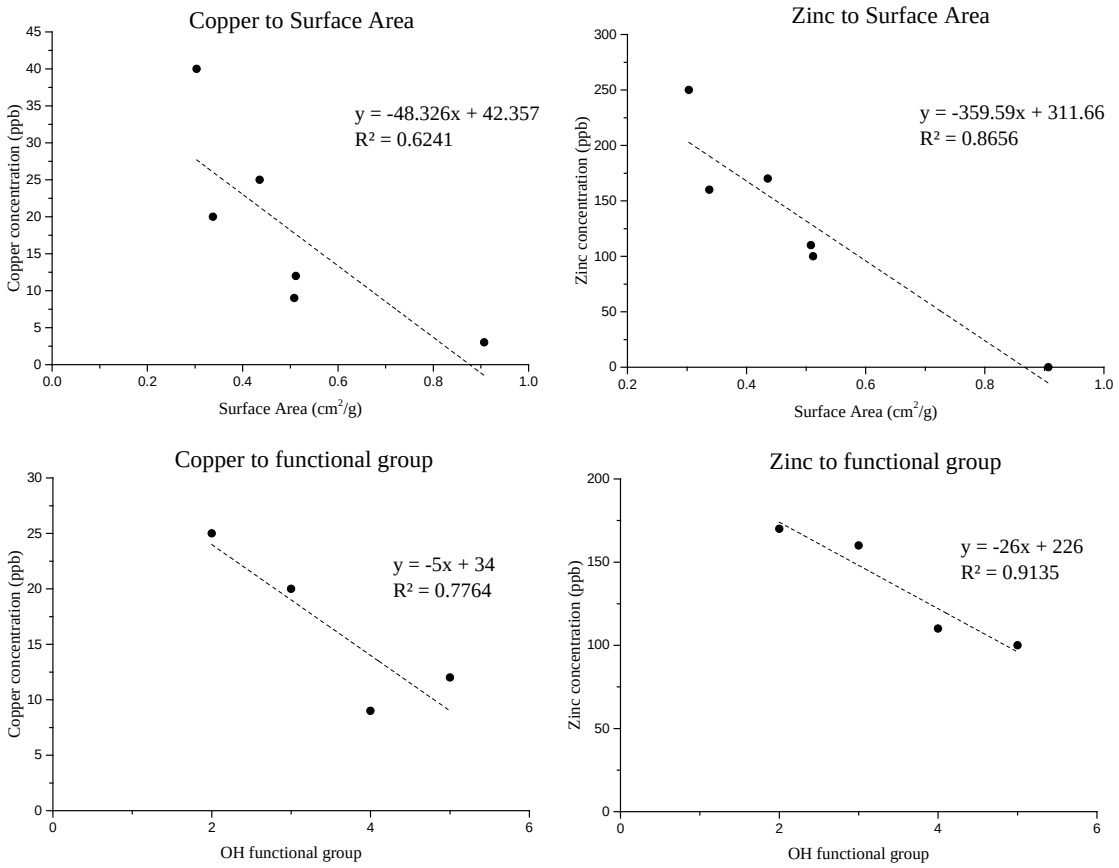

Figure 19. Zinc and copper concentrations in column effluent to the surface area and OH functional group.

3.5.2 Adsorption equilibrium results

Single-solute system

Douglas-fir and ultra-char of Douglas-fir

Figure 20. Comparison of Douglas-fir (R2 = 0.23) and ultra-char of Douglas-fir (R2 = 0.73) for copper adsorption.

and Figure 21. Comparison of Douglas-fir (R2 = 0.88) and ultra-char of Douglas-fir (R2 = 0.81) for zinc adsorption.

show the copper and zinc concentrations in the Douglas-fir and ultra-char of Douglas-fir in a single-solute system, respectively. Figure 20. Comparison of Douglas-fir (R2 = 0.23) and ultra-char of Douglas-fir (R2 = 0.73) for copper adsorption.

shows that copper has a higher affinity for Douglas-fir crumbles than for ultra-char of Douglas-fir, which contradicts the results presented in Figure 13**.** However, Figure 13 shows that this difference in adsorption affinity is minimal. Similarly, the data presented in Figure 21. Comparison of Douglas-fir (R2 = 0.88) and ultra-char of Douglas-fir (R2 = 0.81) for zinc adsorption.

show that zinc also has a greater affinity for Douglas-fir crumbles than for ultra-char of Douglas-fir, which matches the column results (
Figure **16**). These findings indicate that the zinc adsorption mechanism is different from that of copper adsorption for Douglas-fir crumbles and ultra-char of Douglas-fir. In the case of the single-solute system, there is no competition with other solutes, which could show different results compared to the results obtained using a multi-solute system. This outcome may explain the deviation from the column experiments, which are multi-solute tests.

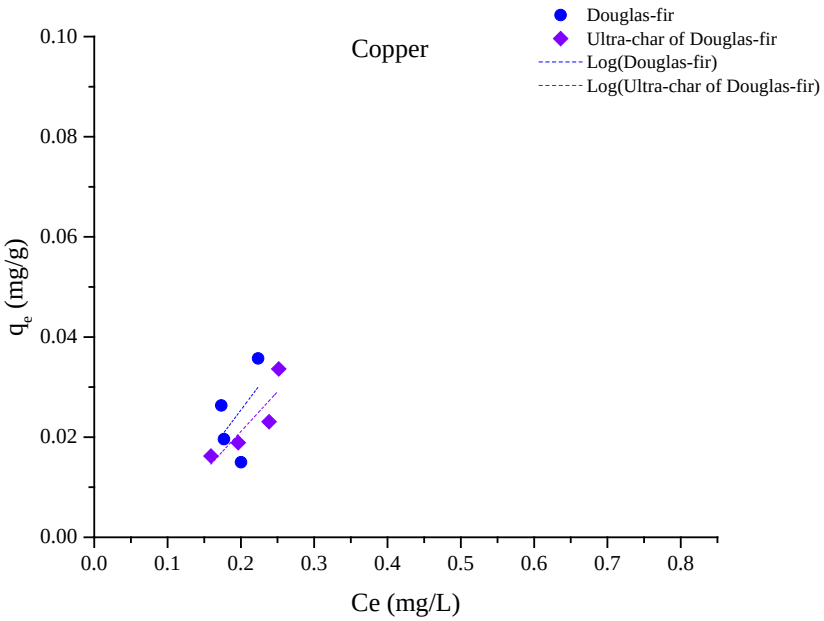

Figure 20. Comparison of Douglas-fir (R^2 = 0.23) and ultra-char of Douglas-fir (R^2 = 0.73) for copper adsorption.

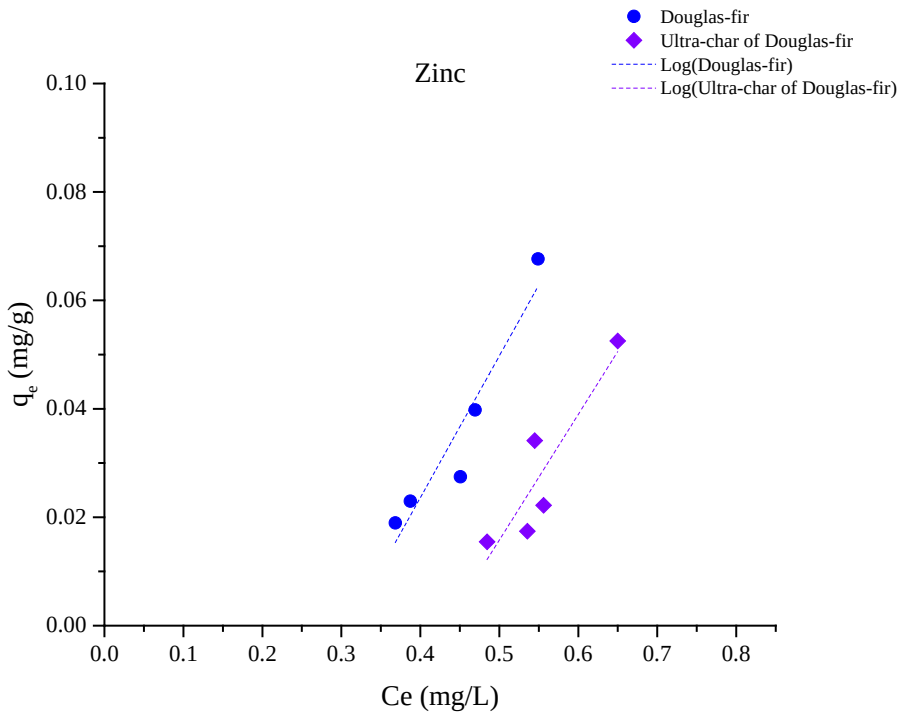

Figure 21. Comparison of Douglas-fir (R^2 = 0.88) and ultra-char of Douglas-fir (R^2 = 0.81) for zinc adsorption.

Poplar and ultra-char of poplar

Figure 22. Comparison of poplar (R2 = 0.06) and ultra-char of poplar (R2 = 0.80) for copper adsorption.

and Figure 23. Comparison of poplar (R2 = 0.44) and ultra-char of poplar (R2 = 0.76) for zinc adsorption.

show the copper and zinc concentrations, respectively, in the poplar crumbles and ultra-char of poplar in a single-solute system.

Figure 22. Comparison of poplar (R2 = 0.06) and ultra-char of poplar (R2 = 0.80) for copper adsorption.

shows that copper has a higher affinity for ultra-char of poplar than for poplar crumbles,

which matches the column test results (Figure 14). These results were anticipated earlier, as ultra-char of poplar has a greater surface area than poplar crumbles (Table 3). Conversely, the data in Figure 23. Comparison of poplar (R2 = 0.44) and ultra-char of poplar (R2 = 0.76) for zinc adsorption.

show that zinc has a greater affinity for poplar crumbles than for ultra-char of poplar, which contradicts the column results presented in Figure 17. This result may be related to the difference between the single-solute and multi-solute systems. This result agrees with results found in the report by Yonge et al. (2016).

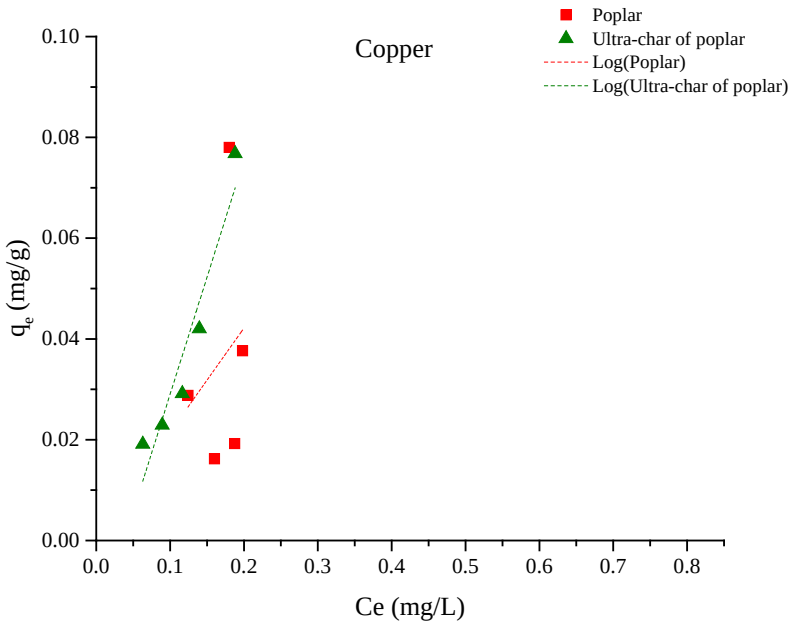

Figure 22. Comparison of poplar (R^2 = 0.06) and ultra-char of poplar (R^2 = 0.80) for copper adsorption.

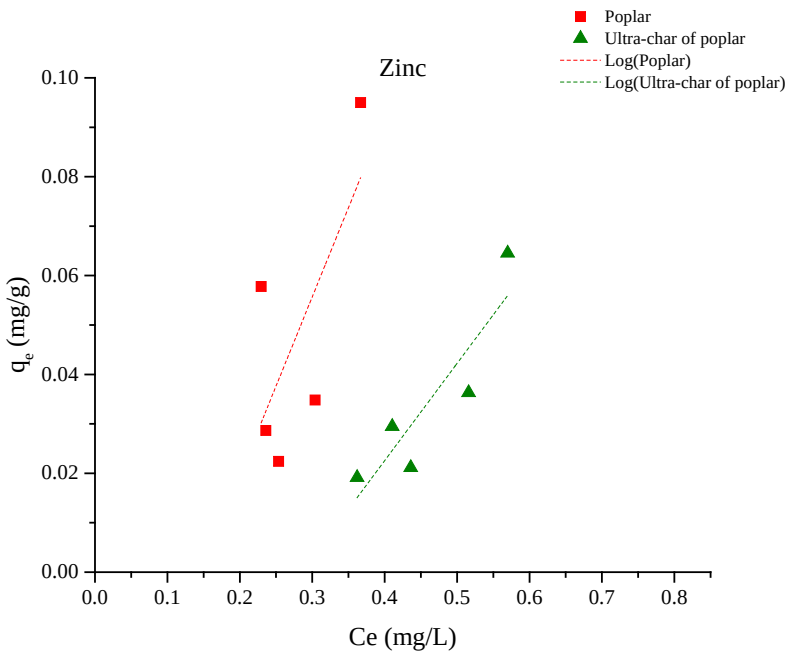

Figure 23. Comparison of poplar (R^2 = 0.44) and ultra-char of poplar (R^2 = 0.76) for zinc adsorption.

Tanoak, lodgepole pine, and ultra-char of alder
Figure 24. Comparison of tanoak (R2 = 0.66), pine (R2 = 0.07), and ultra-char of alder (R2 = 2 x 10-6) for copper adsorption.

and Figure 25. Comparison of tanoak (R2 = 0.27), pine (R2 = 0.58), and ultra-char of alder (R2 = 0.004) for zinc adsorption.

show the copper and zinc concentrations, respectively, in the adsorption equilibrium tests of tanoak, lodgepole pine, and ultra-char of alder in a single-solute system. In the case of the copper concentrations shown in Figure 24. Comparison of tanoak (R2 = 0.66), pine (R2 = 0.07), and ultra-char of alder (R2 = 2 x 10-6) for copper adsorption.

, copper exhibits a higher affinity towards tanoak than for pine and the lowest affinity towards ultra-char of alder. This result was expected, because tanoak has the greatest surface area and the ultra-char of alder has the smallest surface area among these three

kinds of wood (Table 3). These results are also similar to the results shown in **Error! Reference source not found.**. In the case of the zinc concentrations presented in Figure 25. Comparison of tanoak (R2 = 0.27), pine (R2 = 0.58), and ultra-char of alder (R2 = 0.004) for zinc adsorption.

, zinc exhibits a lower adsorption affinity towards the ultra-char of alder, similar to the case for copper adsorption. However, zinc has a higher affinity towards pine than tanoak, unlike the copper adsorption case. Again, these findings suggest that zinc behaves differently from copper towards these samples. These results do not agree with those found by Yonge et al. (2016), which may be due to the difference in organic functional groups between the different materials used in the two studies.

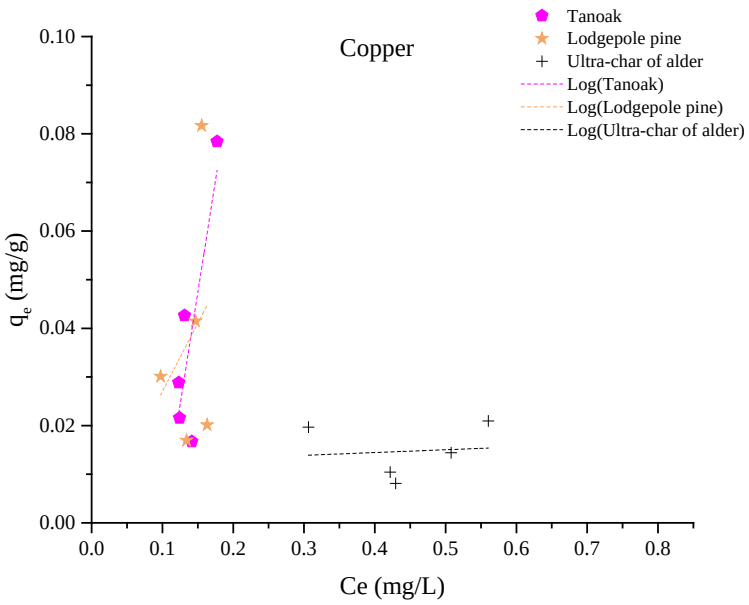

Figure 24. Comparison of tanoak (R^2 = 0.66), pine (R^2 = 0.07), and ultra-char of alder (R^2 = 2 x 10^{-6}) for copper adsorption.

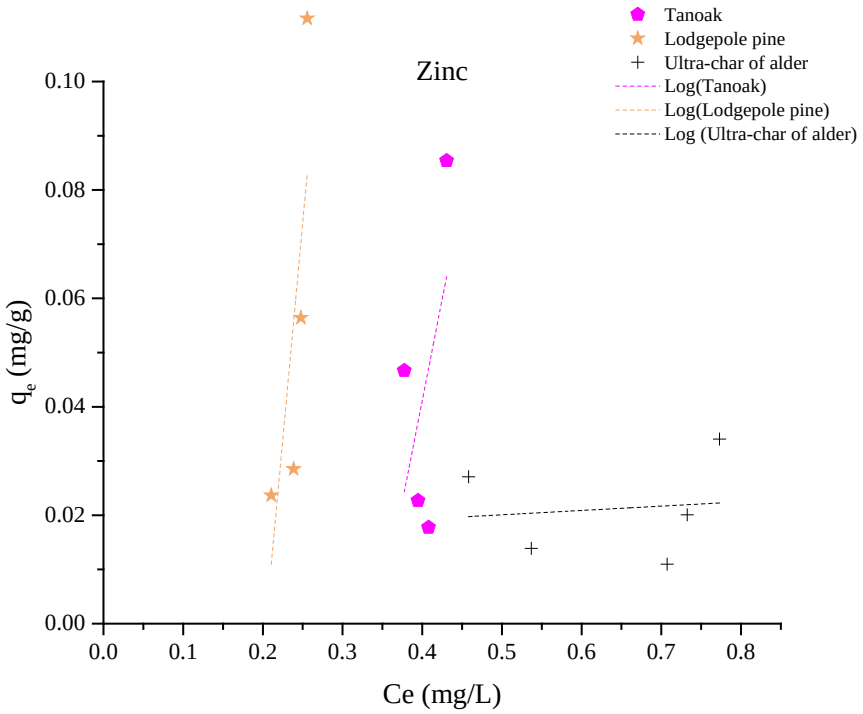

Figure 25. Comparison of tanoak (R^2 = 0.27), pine (R^2 = 0.58), and ultra-char of alder (R^2 = 0.004) for zinc adsorption.

Multi-solute system

Douglas-fir and ultra-char of Douglas-fir

Figure 26. Copper adsorption in Douglas-fir (R2 = 0.89) and ultra-char of Douglas-fir (R2 = 0.78): multi-solute system.

and Figure 27. Zinc adsorption in Douglas-fir (R2 = 0.96) and ultra-char of Douglas-fir (R2 = 0.56): multi-solute system.

show the copper and zinc concentrations, respectively, in Douglas-fir and ultra-char of Douglas-fir in a multi-solute system. In a multi-solute system, there will be competition for adsorption sites between copper and zinc. Figure 26. Copper adsorption in Douglas-fir (R2 = 0.89) and ultra-char of Douglas-fir (R2 = 0.78): multi-solute system.

and Figure 27. Zinc adsorption in Douglas-fir (R2 = 0.96) and ultra-char of Douglas-fir

(R2 = 0.56): multi-solute system.

indicate that copper out-competes zinc for sites of adsorption. Also, copper and zinc adsorption for the Douglas-fir crumbles remained almost the same, but for the ultra-char of Douglas-fir, the copper adsorption seems greater than the zinc adsorption. These results agree with the (Yonge et al. 2016) study.

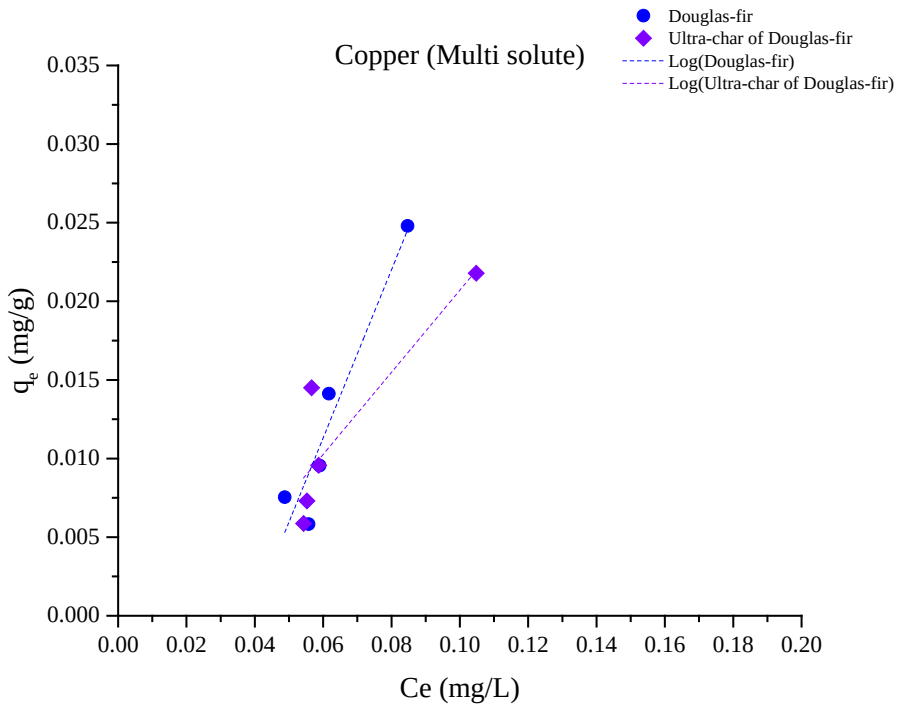

Figure 26. Copper adsorption in Douglas-fir (R^2 = 0.89) and ultra-char of Douglas-fir (R^2 = 0.78): multi-solute system.

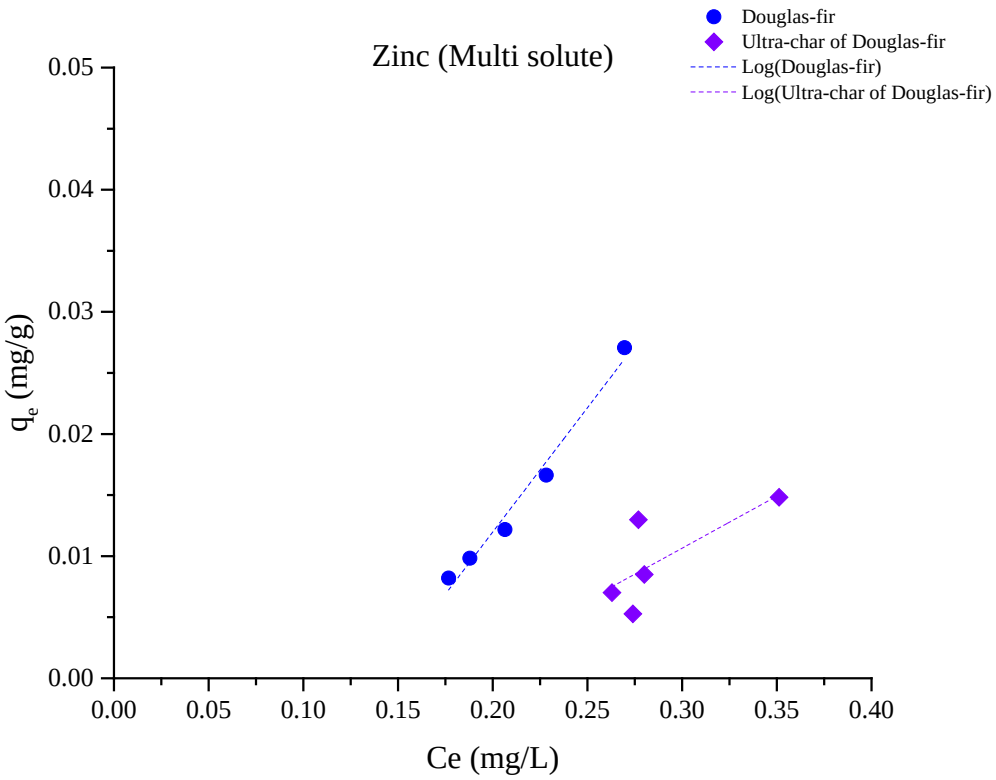

Figure 27. Zinc adsorption in Douglas-fir (R^2 = 0.96) and ultra-char of Douglas-fir (R^2 = 0.56): multi-solute system.

Poplar and ultra-char of poplar

Figure 28. Copper adsorption in poplar (R2 = 0.26) and ultra-char of poplar (R2 = 0.73): multi-solute system.

and Figure 29. Zinc adsorption in poplar (R2 = 0.49) and ultra-char of poplar (R2 = 0.75): multi-solute system. show the copper and zinc concentrations, respectively, in the poplar crumbles and ultra-char of poplar in a multi-solute system. Both figures show that copper and zinc adsorption for the ultra-char of poplar remained almost the same, but for the poplar crumbles, the zinc adsorption seems greater than the copper adsorption. This finding is similar to that for the single-solute system as well (

Figure 22. Comparison of poplar (R2 = 0.06) and ultra-char of poplar (R2 = 0.80) for copper

adsorption.

and Figure 23. Comparison of poplar (R2 = 0.44) and ultra-char of poplar (R2 = 0.76) for zinc adsorption.

).

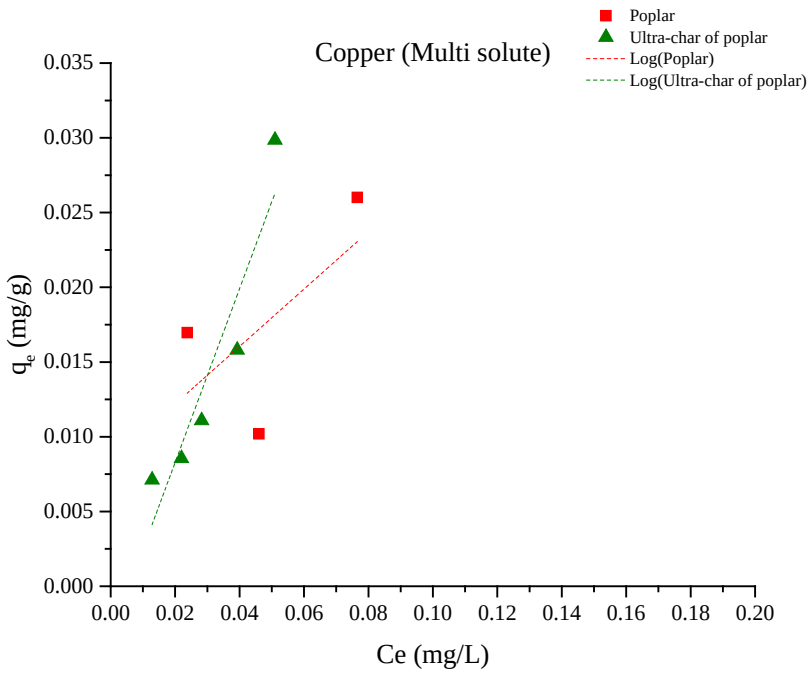

Figure 28. Copper adsorption in poplar (R^2 = 0.26) and ultra-char of poplar (R^2 = 0.73): multi-solute system.

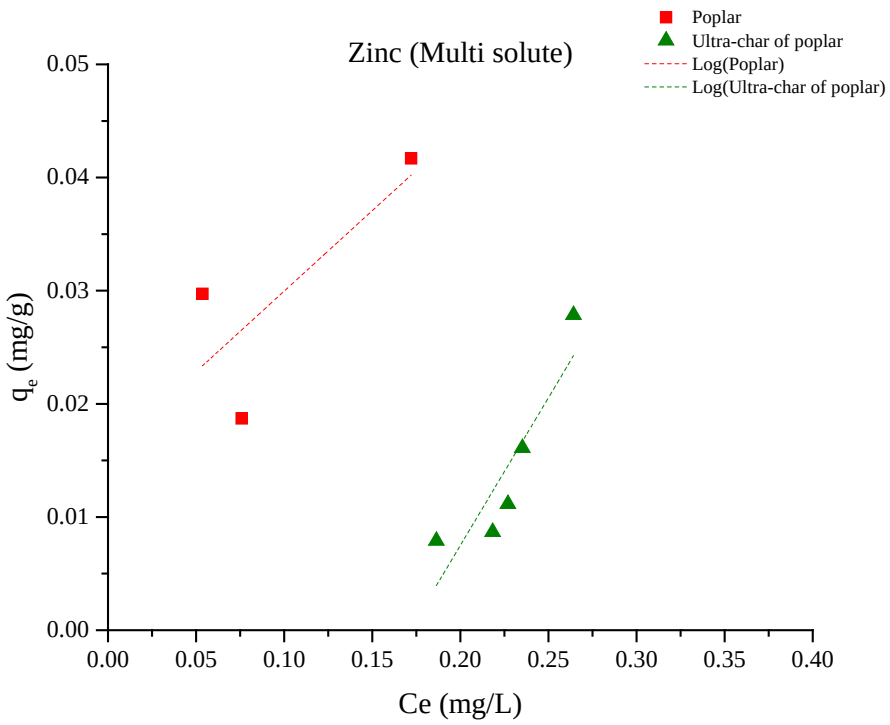

Figure 29. Zinc adsorption in poplar (R^2 = 0.49) and ultra-char of poplar (R^2 = 0.75): multi-solute system.

Tanoak, lodgepole pine, and ultra-char of alder

Figure 30. Copper adsorption in tanoak (R2 = 0.98), pine (R2 = 0.002), and ultra-char of alder (R2 = 0.02): multi-solute system.

and Figure 31. Zinc adsorption in tanoak (R^2 = 0.52), pine (R^2 = 0.17), and ultra-char of alder (R^2 = 0.009): multi-solute system.

show the copper and zinc concentrations, respectively, for tanoak, lodgepole pine, and ultra-char of alder in a multi-solute system. The order (ranking) of the adsorption capacity for both copper and zinc in tanoak, pine, and ultra-char of alder in a multi-solute system remained essentially the same as in the single-solute system. However, for tanoak, the zinc adsorption lessened in the multi-solute system, and for pine, the copper adsorption lessened in the multi-solute system compared to the single-solute system. Most of the results from the multi-solute experiments agree with those of the Yonge et al. (2016) study.

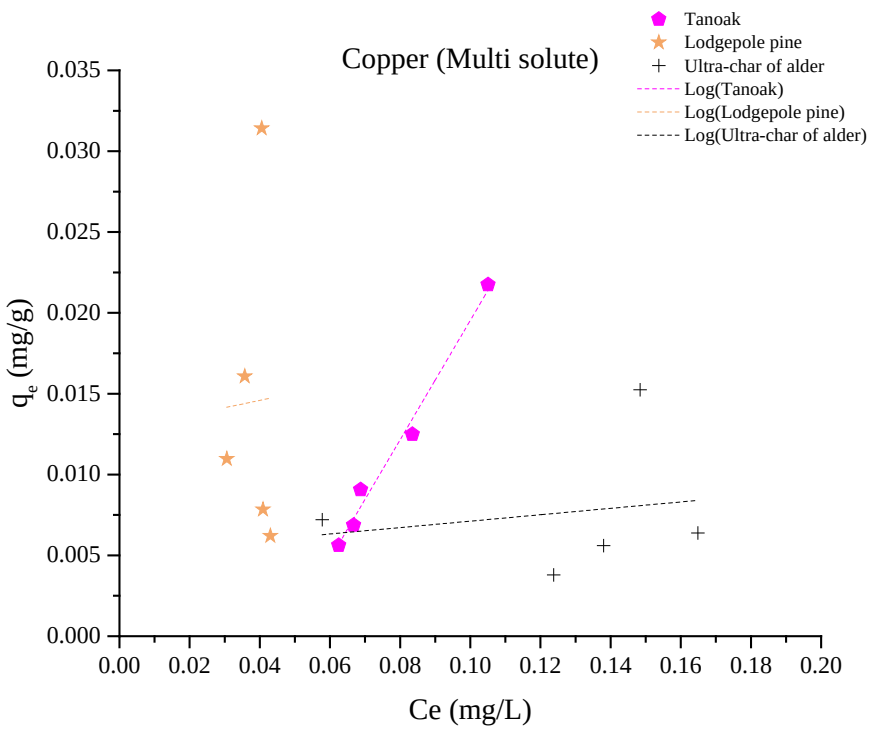

Figure 30. Copper adsorption in tanoak (R^2 = 0.98), pine (R^2 = 0.002), and ultra-char of alder (R^2 = 0.02): multi-solute system.

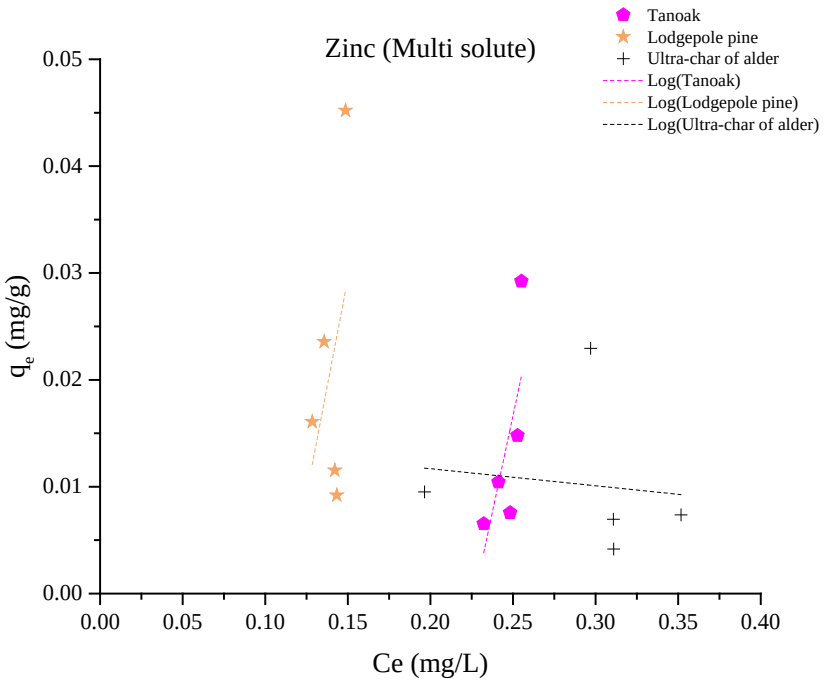

Figure 31. Zinc adsorption in tanoak (R^2 = 0.52), pine (R^2 = 0.17), and ultra-char of alder (R^2 = 0.009): multi-solute system.

The results from the batch experiments discussed above for both single-solute and multi-solute systems indicate that tanoak might be the best choice for copper and zinc adsorption, unlike the ultra-char of poplar that was determined to be the best choice in the column tests.

4. Summary and Conclusions

Based on both the column experiments and batch adsorption tests, one of the most important conclusions that can be drawn from this study is that the surface areas of both wood crumbles and ultra-char of different wood crumbles are highly relevant to their ability to adsorb copper and zinc. Media with greater surface areas are advantageous in heavy metal adsorption. The role of functional groups is not as important as we had anticipated.

Table 4 represents a summary of the overall findings. Among all the samples of wood crumbles and char, tanoak crumbles seem to be the best option for metal adsorption. Under all the conditions, including column experiments and batch adsorption tests in both single- and multi-solute conditions, the tanoak crumbles showed good adsorption ability (Table 4). The surface areas of tanoak crumbles are in the midrange among all the samples (Table 3). The strength ranking of the OH functional groups is as follows: poplar > tanoak > Douglas-fir > lodgepole pine. More OH functional groups in the filtration media resulted in greater adsorption of copper and zinc. As the tanoak crumbles show relatively high OH strength,

we can infer that tanoak would be the best choice for copper and zinc removal among the tested wood crumbles. Moreover, as tannins (Figure 6) are usually found in tanoak (Bowcutt 2015), they could be the reason for the good copper and zinc adsorption of tanoak crumbles.

Table 4. Ranking of Performance in Batch Adsorption Tests and Column Tests (High to Low)

Single-solute system		Multi-solute system		Column tests	
Copper	**Zinc**	**Copper**	**Zinc**	**Copper**	**Zinc**
Tanoak	Lodgepole pine	Douglas-fir	Tanoak	Ultra-char of poplar	Ultra-char of poplar
Ultra-char of poplar	Tanoak	Tanoak	Lodgepole pine	Tanoak	Tanoak
Lodgepole pine	Poplar	Ultra-char of Douglas-fir	Ultra-char of poplar	Poplar	Poplar
Ultra-char of Douglas-fir	Ultra-char of Douglas-fir	Ultra-char of poplar	Douglas-fir	Ultra-char of Douglas-fir	Douglas-fir
Poplar	Douglas-fir	Poplar	Ultra-char of Douglas-fir	Douglas-fir	Lodgepole pine
Douglas-fir	Ultra-char of poplar	Lodgepole pine	Poplar	Lodgepole pine	Ultra-char of Douglas-fir
Ultra-char of alder	Ultra-char of alder	Ultra-char of alder	Ultra-char of alder	Ultra-char of alder	Ultra-char of alder

Among the ultra-chars of the different wood crumbles, poplar char seems to be the best option for metal adsorption. It has a relatively large surface area (Table 3) and exhibits much better adsorption than the other chars (Table 4). However, ultra-chars have fewer OH functional groups, indicating that ultra-chars can remove copper and zinc better than other media due to their greater surface areas. Alder char showed the least adsorption of copper and zinc under all conditions (Table 4). Alder char has the smallest surface area and OH functional groups among all the samples (Table 3).

The results clearly indicate that the metal adsorption of wood crumbles and ultra-chars of different wood crumbles is related to different operating parameters and media properties, such as surface areas and functional groups. The mixed results suggest that we may be able to design blends (ratios of various species and char/raw) to optimize system performance.

The overall results indicate that surface areas may be a more important parameter for the adsorption of copper and zinc than functional groups, which proved to be not as important as initially expected. The reason that raw wood samples showed better adsorption in the previous study (Yonge et al. 2016) may be due to the difference in both the surface areas and functional groups in the filtration media. Usually, biochars have greater surface areas and fewer functional groups than wood crumbles. Functional groups would be advantageous for metal adsorption when two materials have similar surface areas, which may be the reason for the better adsorption of copper and zinc using raw wood crumbles over biochar that was found in the previous Yonge et al. (2016) study.

In a future study, the temperature used to make biochar should be used as a variable. A wealth of published literature is available about the quality of biochar as a function of the pyrolysis temperature; that is, a relatively large surface area and activation potential correspond to an increase in production temperature (Mohan, Pittman, and Steele 2006).

5. Applications for the Ferry Terminal

Findings from this study will be helpful for selecting appropriate filtration medium for removal of heavy metals at a ferry terminal. Overall our study shows that tanoak crumbles will be a suitable filtration medium. Tanoak crumbles could be deployed in a catch basin as filtration medium following the same process mentioned in our last report by Yonge et al. (2016). In the Yonge et al. (2016) study, the Bainbridge Island ferry terminal was selected as the field test site. The catchment used in this project was a paved, 1.5-acre, vehicle staging area set aside for traffic waiting to board the ferry. A pilot scale adsorption column and submersible weir system was designed and constructed to fit within an existing stormwater vault. During each storm event, the column's design allowed stormwater to enter laterally through the top of the column, pass vertically downward through the media, and exit to the submersible weir that was used to determine flow. We recommend a similar process for testing and applications of tanoak crumbles as a filtration medium at the ferry terminal. The filtration media will be packed in a field-scale adsorption column. The column will be filled with tanoak crumbles sandwiched between pea gravel. The packed column will be deployed in a catch basin as a filtration medium. However, field-scale study is needed to determine the effectiveness of tanoak media for stormwater treatment in the ferry terminal. Field study will also provide us information on the longevity of stormwater treatment without replacing the tanoak medium. Furthermore, selection of appropriate media will also be dependent on the economic trade-offs in using one medium in preference to another. Hence, future study should include the economic analysis of selection of filtration media for stormwater treatment in the ferry terminal.

References

Ameloot, Nele, Ellen R Graber, Frank GA Verheijen, and Stefaan De Neve. 2013. 'Interactions between biochar stability and soil organisms: review and research needs', *European Journal of Soil Science*, 64: 379-90.

Angerville, Ruth, Yves Perrodin, Christine Bazin, and Evens Emmanuel. 2013. 'Evaluation of ecotoxicological risks related to the discharge of combined sewer overflows (CSOs) in a periurban river', *International journal of environmental research and public health*, 10: 2670-87.

Bowcutt, Frederica. 2015. *The Tanoak Tree: An Environmental History of a Pacific Coast Hardwood* (University of Washington Press).

Brooks, Kenneth M, and Conrad VW Mahnken. 2003. 'Interactions of Atlantic salmon in the Pacific northwest environment: II. Organic wastes', *Fisheries Research*, 62: 255-93.

Brown, Jeffrey N., and Barrie M. Peake. 2006. 'Sources of heavy metals and polycyclic aromatic hydrocarbons in urban stormwater runoff', *Science of The Total Environment*, 359: 145-55.

Burton Jr, G Allen, and Robert Pitt. 2001. *Stormwater effects handbook: A toolbox for watershed managers, scientists, and engineers* (CRC Press).

Chen, J Paul, and Xiaoyuan Wang. 2000. 'Removing copper, zinc, and lead ion by granular activated carbon in pretreated fixed-bed columns', *Separation and Purification Technology*, 19: 157-67.

Chen, Xincai, Guangcun Chen, Linggui Chen, Yingxu Chen, Johannes Lehmann, Murray B McBride, and Anthony G Hay. 2011. 'Adsorption of copper and zinc by biochars produced from pyrolysis of hardwood and corn straw in aqueous solution', *Bioresource technology*, 102: 8877-84.

Colom, X, F Carrillo, F Nogués, and P Garriga. 2003. 'Structural analysis of photodegraded wood by means of FTIR spectroscopy', *Polymer degradation and stability*, 80: 543-49.

Council, National Research. 2009. *Urban stormwater management in the United States* (National Academies Press).

Davis, Allen P, Mohammad Shokouhian, and Shubei Ni. 2001. 'Loading estimates of lead, copper, cadmium, and zinc in urban runoff from specific sources', *Chemosphere*, 44: 997-1009.

Demirbas, Ayhan. 2008. 'Heavy metal adsorption onto agro-based waste materials: a review', *Journal of hazardous materials*, 157: 220-29.

Dooley, James H., David N. Lanning, and Christopher J. Lanning. 2013. 'Woody biomass size reduction with selective material orientation', *Biofuels*, 4: 35-43.

Gangolli, SD. 2007. *The dictionary of substances and their effects (DOSE)* (Royal Society of chemistry).

Mahrosh, Urma, Merethe Kleiven, Sondre Meland, Bjørn Olav Rosseland, Brit Salbu, and Hans-Christian Teien. 2014. 'Toxicity of road deicing salt (NaCl) and copper (Cu) to fertilization and early developmental stages of Atlantic salmon (Salmo salar)', *Journal of hazardous materials*, 280: 331-39.

Mohan, Dinesh, Charles U Pittman, and Philip H Steele. 2006. 'Pyrolysis of wood/biomass for bio-oil: a critical review', *Energy & fuels*, 20: 848-89.

Mohan, Dinesh, Ankur Sarswat, Yong Sik Ok, and Charles U Pittman. 2014. 'Organic and inorganic contaminants removal from water with biochar, a renewable, low cost and sustainable adsorbent–a critical review', *Bioresource technology*, 160: 191-202.

Park, Junyeong, Jiajia Meng, Kwang Hun Lim, Orlando J Rojas, and Sunkyu Park. 2013. 'Transformation of lignocellulosic biomass during torrefaction', *Journal of Analytical and Applied Pyrolysis*, 100: 199-206.

Pitcher, S. K., R. C. T. Slade, and N. I. Ward. 2004. 'Heavy metal removal from motorway stormwater using zeolites', *Science of The Total Environment*, 334: 161-66.

Reynolds, Tom D Richards, Paul A Tom D Reynolds, and Paul A Richards. 1996. 'Unit operations and processes in environmental engineering', *PWS series in engineering.*

Skidmore, JF. 1964. 'Toxicity of zinc compounds to aquatic animals, with special reference to fish', *The quarterly review of Biology*, 39: 227-48.

Walker, William J, Richard P McNutt, and CarolAnn K Maslanka. 1999. 'The potential contribution of urban runoff to surface sediments of the Passaic River: sources and chemical characteristics', *Chemosphere*, 38: 363-77.

Willson, Mary F, and Karl C Halupka. 1995. 'Anadromous fish as keystone species in vertebrate communities', *Conservation Biology*, 9: 489-97.

Yonge, David, Vince McIntyre, Joseph Smith, Ian Norgaard, and Michael Wolcott. 2016. "Sustainable Design Guidelines to Support the Washington State Ferries Terminal Design Manual: Assessment of Copper and Zinc Adsorption to Lignocellulosic Filtration Media Using Laboratory and Field Scale Column Tests for the Purpose of Urban Stormwater Remediation." In.

Yonge, David, and Piper Roelen. 2003. "An evaluation of stormwater permeable rapid infiltration barriers for use in class V stormwater injection wells." In.

Americans with Disabilities Act (ADA) Information:
This material can be made available in an alternate format by emailing the Office of Equal Opportunity at wsdotada@wsdot.wa.gov or by calling toll free, 855-362-4ADA(4232). Persons who are deaf or hard of hearing may make a request by calling the Washington State Relay at 711.

Title VI Statement to Public:
It is the Washington State Department of Transportation's (WSDOT) policy to assure that no person shall, on the grounds of race, color, national origin or sex, as provided by Title VI of the Civil Rights Act of 1964, be excluded from participation in, be denied the benefits of, or be otherwise discriminated against under any of its federally funded programs and activities. Any person who believes his/her Title VI protection has been violated, may file a complaint with WSDOT's Office of Equal Opportunity (OEO). For additional information regarding Title VI complaint procedures and/or information regarding our non-discrimination obligations, please contact OEO's Title VI Coordinator at (360) 705-7082.